Addis Ababa University

College of Natural and Computational Sciences

School of Earth Sciences

Integrated geophysical approaches for geothermal potential assessment of the Arto hot spring, Alaba Woreda, Southern Ethiopia.

A thesis is submitted to the School of Graduate Studies of Addis Ababa University in partial fulfillment of the requirements for the degree of Master of Science in Applied Geophysics.

By: Wubayehu Dessalegn

Addis Ababa

June 2020

ADDIS ABABA UNIVERSITY
SCHOOL OF GRADUATE STUDIES
SCHOOL OF EARTH SCIENCES

This is to certify that the thesis prepared by Wubayehu Dessalegn, entitles: "**Integrated geophysical approaches for geothermal potential assessment of the Arto Hot spring, Alaba Woreda, Southern Ethiopia"** and submitted in partial fulfillment of the requirements for the degree of Master of Science in Applied Geophysics complies with the regulations of the University and meets the accepted standards with respect to originality and quality.

Approved by the board of examiners:

Dr. Balemual Atinafu	_____	_____
Chairman, School of Earth sciences	Signature	Date
Prof. Tigistu Haile	_____	_____
Advisor	Signature	Date
Prof. Gezahegn Yirgu	_____	_____
Co-advisor	Signature	Date
Prof. Tilahun Mamo	_____	_____
Internal examiner	Signature	Date
Dr. Ameha Atinafu	_____	_____
External examiner	Signature	Date

Abstract

In this research, integrated geophysical survey using electrical and magnetic methods was conducted to assess the geothermal energy potential of the Arto hot spring, Alaba special zone, southern Ethiopia. The study area is located 240km southward from Addis Ababa, and accessible through the Ziwaw - Shasemene- Alaba asphalt road. In Ethiopia, there exist some geothermal energy prospects, which have proved to have significant geothermal potential. Arto hot spring is one of the geothermal sites, about which prospection had not been carried out, yet. The main objective of the research is assessing the geothermal potential of the area, Arto hot spring, by employing geophysical methods, apart from describing geological features (both structures & lithology), and geothermal manifestations, such as hot springs, mud pool and swamps.

Totally, the geophysical data has been gathered at -nine vertical electrical sounding (VES) data points using Schlumberger electrode array with a maximum half electrode spacing, AB/2=750m in three traverse lines; and 311magnetic data points with station spacing 10m. The analysis result of the resistivity data was presented in the form of interpreted VES curves, pseudo depth section, stacked section, and geoelectric section maps. Whereas the magnetic data was presented in terms of total magnetic, residual magnetic anomaly, analytical signal, tilt derivative, Euler deconvolution magnetic and magnetic profile maps.

From the electrical resistivity analysis, the low resistivity, which is less than 10Ω-m, and observed on the pseudo depth & geoelectric sections along Line-1, depicts that the geothermal manifestations. The result indicates that the low resistivity is due to the combined effects of the lithology of the subsurface rocks, the thermal heat, and the high salinity of the subsurface fluid. In the analysis, low magnetic anomaly coincides with low electrical resistivity results, showing that there exists anomalous subsurface heat. The magnetic anomaly map depicts the subsurface geological structures, trending NE-SW and NW-SE. The dominant structures, observed in the study area is correspondingly aligned with the general trend of the Main Ethiopian Rift (i.e., NE - SW). The main thermal manifestations in the study area are situated parallel with the Main Ethiopian Rift structure.

According to the result acquired from the geophysical methods and the thermal manifestations, the area is proved to be potential from geothermal energy resource point of view. However, more detailed-geophysical surveys should be conducted.

Acknowledgment

Firstly, I would like to give my sincere gratitude to Addis Ababa University, the School of Earth Sciences for providing me the opportunity to attend the postgraduate program, and funding the research project.

I would also like to express my heartfelt gratitude to my advisors, prof. Tigistu Haile and co-advisor prof. Gezahegn Yirgu, for their unreserved guidance, suggestion and advice, as well as the support in collecting the field data.

My gratefully thank goes to Dr. Balemwal Atinafu, head of the School of Earth Sciences of Addis Ababa University, for his priceless help in arranging the fieldwork.

I express my deep gratitude to my classmate student, Esubalew Yehalaw, for his support in collecting the primary data in the field. I would like to express my grateful thanks to my colleagues, Bekelu Abebe and Wubamilak Ngusse, for their cooperation in the data processing phase.

I am thankful to Alaba woreda water, irrigation and energy office; and the local community of Tachignaw Arsho for their cooperation during the fieldwork.

Lastly, but not least, my thank goes to Mr. Fisiha Genetu, my husband, for his consistent encouragement and endless help in reviewing the work. I am also thankful to my family members.

Contents

List of Figures

List of Tables

Acronyms

2D	Two-dimensional
3D	Three-dimensional
a.s.l	Above sea level
CMER	Central Main Ethiopian Rift
DC	Direct current
EARS	East Africa Rift system
EIGS	Ethiopian Institute of Geological Survey
IGRF	International Geomagnetic Reference Field
GPS	Global Positioning System
MER	Main Ethiopian Rift
MT	Magnetotelleric
NE-SW	Northeast- southwest
NNE-SSW	North northeast – south southwest
NW-SE	Northwest – southeast
nT	Nano Tesla
SI	Structural Index
TDS	Total Dissolved Solids
TEM	Transit electromagnetic methods
UNDP	United Nations Development Program
UTM	Universal Transverse Mercator
VES	Vertical electrical sounding
WFB	Wonji Fault Belt
Ω-m	Ohm-meter
°C	Degree Celsius

CHAPTER ONE

1 INTRODUCTION

1.1 Background

Energy is an essential resource in Ethiopia's development strategy because it is a catalyst for industrial progress and a source of foreign exchange. Although Ethiopia has a diversity of potential energy resources (hydropower, geothermal, wind, solar and natural gas), it currently relies for power generation on hydropower resources as well as imported petroleum and petroleum products (Teklemariam et al., 2000).

Geothermal energy, amongst the natural sources of energy available to mankind, is the heat energy produced within the Earth subsurface. It is the form of clean, reliable, and renewable energy resource. Geothermal energy is an efficient heating and cooling alternative for residential, commercial, and industrial applications, and is potentially a significant source for electrical power generation.

Geothermal energy could be expressed as the heat generated within the Earth, which could be exploited for different use according to the amount of temperature that is produced. Geothermal resources, according to Mary and Mario (2004), are generally associated with tectonically active regions that are generated because of plate movements and volcanic activities. It results because of temperature differences between the different parts of the asthenosphere where convective movements are formed. This slow convective movement is said to be maintained by the radioactive elements and heat from the deepest part of the Earth. The less dense, deep hotter rocks tend to rise along with the movement towards the surface while the colder but heavier rocks close to the surface tend to sink, re-heat and rise again. Figure 1.1 gives a schematic representation of a typical geothermal system.

The geological setting in which a geothermal reservoir is to be found can vary widely (Fitch A.A, 1981). The geothermal fields currently may occur in rocks that range from limestone to shale, volcanic rock and granite. Volcanic rocks are probably the most rock type in which reservoirs occur. The geothermal reservoirs may occur in convection systems in which hot water rises from deep within the earth and trapped in reservoirs whose cap rock have been formed by

silicification, or precipitation of other mineral elements. According to Manzella (2000), the important factors in identifying a geotherma1 reservoir are not rock units, but rather the existence of tectonic elements such as fracturing, and the presence of high heat flow.

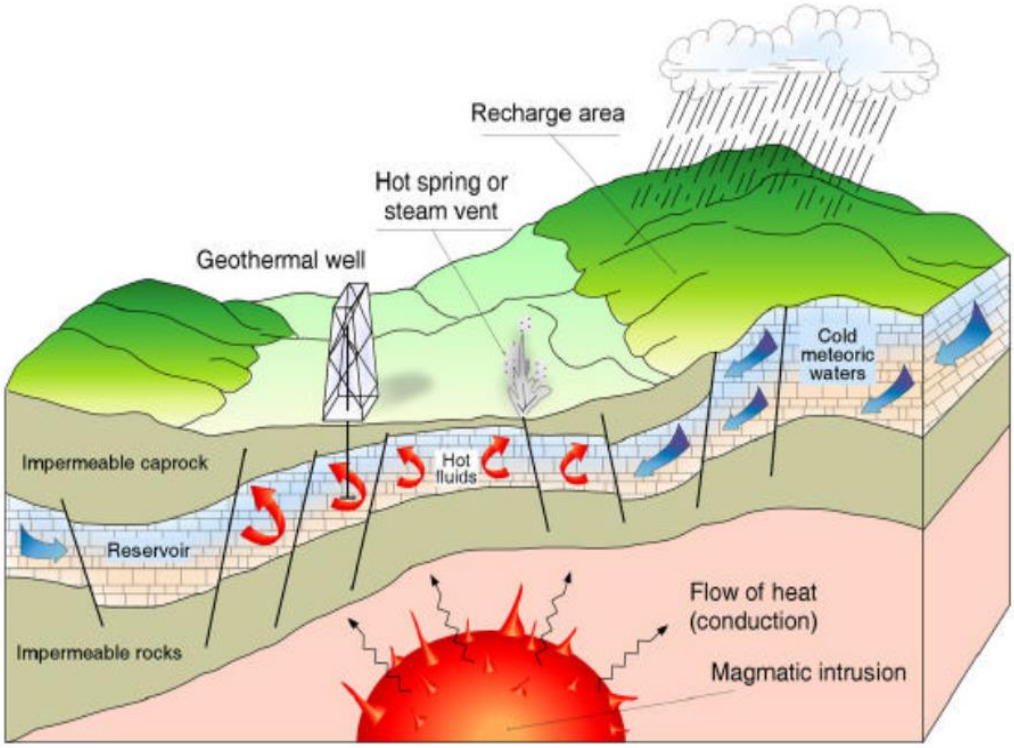

Figure 1.1 Schematic representation of an ideal geothermal system (Kana et al., 2015)

Ethiopia is one of few countries in Africa, known to have a significant amount of geothermal resources. These resources are found scattered in the Ethiopian Rift valley and in the Afar Depression, which are both part of the East African Rift System (EARS). More than sixteen geothermal prospects that are believed to have the potential for electricity production are located along the Rift. Abaya, Aluto Langano, Tendaho, Corbetti, Tulumoye-Gedemsa, Dofan and Fantale are a few of the prospect areas in which detailed exploration study and drilling have started due to their expected potential (Selamawit Worku,2016). According Meseret Teklemariam and Kibret Beyene (2005), Ethiopia could possibly generate more than 1,000 MWe of electric power from geothermal resources. Some of the well-known geothermal manifestation and potential areas in the Main Ethiopian Rift are shown in Figure 1.2.

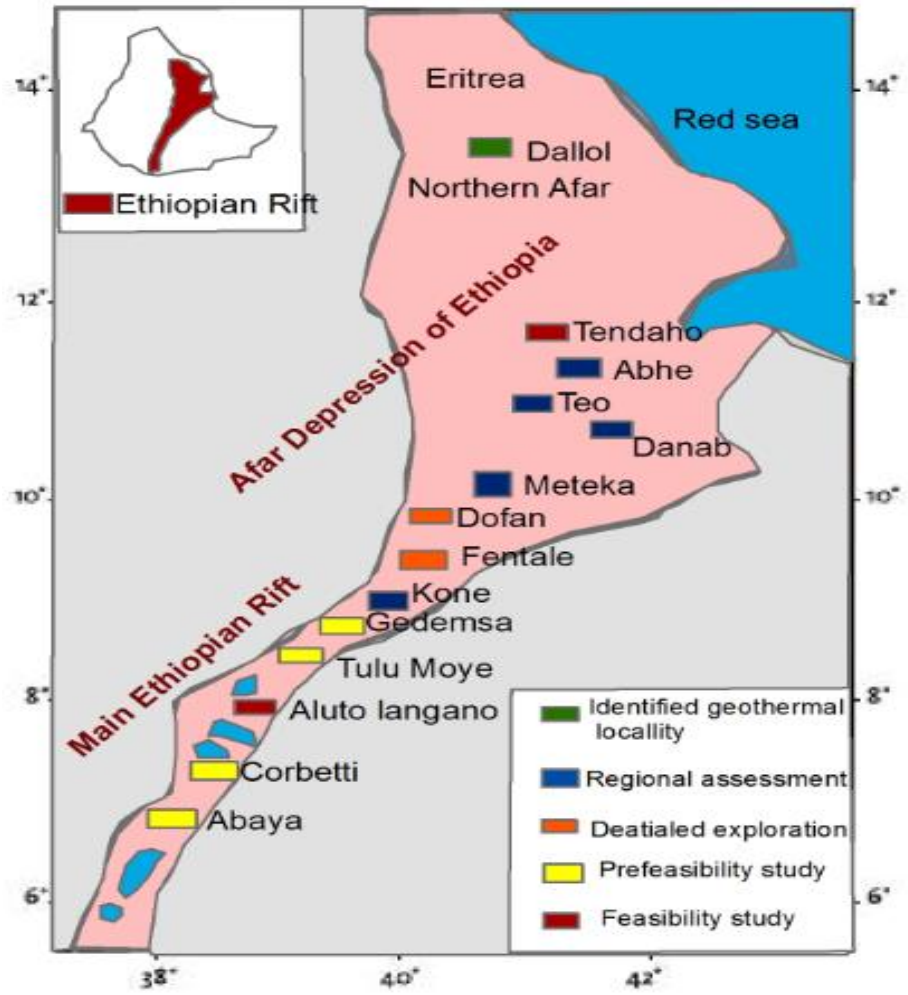

Figure 1.2 Geothermal manifestations and potential area for geothermal resource study in the Main Ethiopian Rift, (MER) (Meseret Teklemariam., 2006)

There are several ways to explore geothermal resource and amongst the many methods that could be used to investigate geothermal resource and potential of a particular site, geophysical surveys form an important part. Geophysical methods play a key role in geothermal exploration since many objectives of geothermal study could be achieved by these methods. Geophysical surveys obtain the physical parameter of the geothermal system, indirectly, from the surface or measurements at from shallow depth. In essence, geophysical methods are applied to obtain information about the subsurface of the Earth that is not available from surface geological observations. The application of geophysical field surveys enables one to detect and map

underground inhomogeneity and structures to solve various problems in the field of applied geology and engineering. Applying such methods, particularly, for the evaluation of hydrogeological systems has a great role.

The hot spring in the study area is manifested in the NE-SW direction with water temperatures ranging between 70°C-94°C (mean 82°C). It is possible to observe four major active-thermal spring spots, from which one of it is the mud pool with the highest temperature. The local people used the thermal heat for traditionally medication purpose and prepared food (like hot drink, potato and maize). The hot spring may be discharge through the weak zone, which aligned to the Main Ethiopian Rift (MER) structure. The area is geologically characterized by quaternary volcanic rock with fractured ignimbrite, tuff and ash rocks.

A number of studies have been conducted to investigate thermal manifestation areas in the MER. The thermal manifestations close to Alaba town, specifically, at the locality of Arto hot spring, however, has not been subjected yet to detailed prospection and the existence of a large potential geothermal energy resource had not been carried out. The main objective of this research work is, therefore, to study this less known geothermal manifestation site and delineate the existence of a geothermal system and geological structures that control flow of geothermal fluids and to identify the geothermal system (shallow depth heat and fluid interaction zone) in Arto hot spring.

1.2 Location and accessibility of the study area

The study area is located in the Main Ethiopian Rift (MER) in the South Nations Nationalities and Peoples Regional State, Alaba Woreda, specifically, at the locality of the Arto hot spring. The site is situated at about 240 km from Addis Ababa (Figure 1.3). It is accessed either (1) by an asphalt road running from Addis Ababa and passing through Ziway and Shashemene towns to Alaba town; or (2) using an asphalt road, too, joining Addis Ababa city through Butajira-Worabe- Alaba towns.

The Arto hot spring is, specifically, situated in the Bilate river catchment at about 10 Km from Alaba town in the southwest direction, following an all-weather gravel road. It is bounded between a UTM coordinates of [391000 – 398500] m easting and [804000 – 808608] m northing.

The flat lying ground of the hot spring area is found at an elevation of 1775m above mean sea level

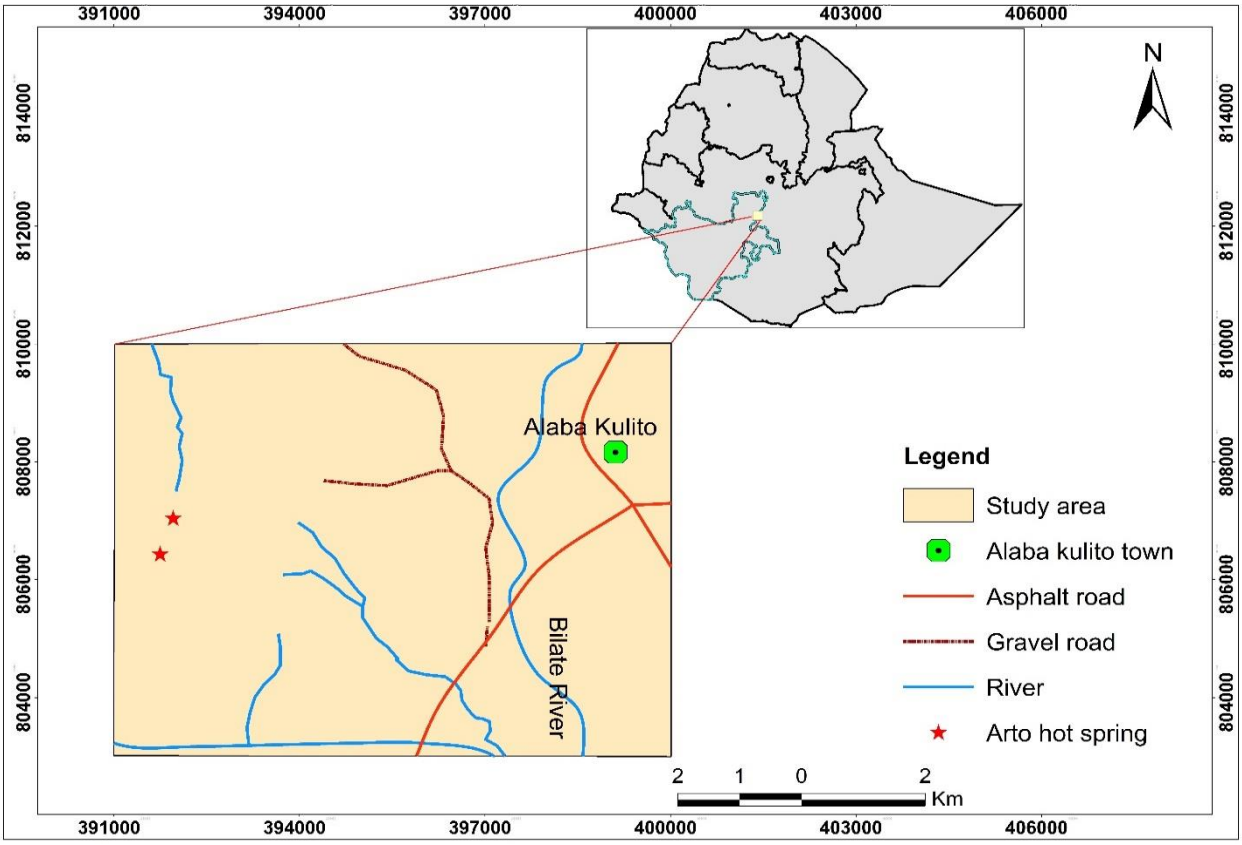

Figure 1.3 Location map of the study area

1.3 Physiography and drainage of the study area

The study area is found in Bilate river catchment at elevation of 1775 meter above mean sea level. The Bilate river catchment have been three main perennial rivers such as Bilate, Gidabo and Gelana that flow into the Lake Abaya. Topographically the basin is characterized by low land pain area to highly rugged and mountainous terrain.

The western part of the study area is characterized by rugged and mountains ridge, surrounded by Mt. Dato highland at elevation of 2460 meter above mean sea level. Generally, the study area is somehow flat land and affected by erosional process especially the elevated grounds on the north and northwestern sides (Figure 1.4).

The thermal waters from the number of hot springs and mud sprouts form large size mud pool and thermal pond from which a large discharge stream flows southwards. The local population and people coming from afar use the hot springs as thermal healing and on a normal day one would always see a good number of people around the number of hot spots and on a number of locations following the stream. This stream flows into Bilate River, which is the perennial river in the study area that flows from Gurage Mountains to the Lake Abaya.

On its south and southeastern side, the rift floor comprises of flat volcano sedimentary plains at an average altitude of 1700 m a.s.l and is characterized by a series of sub-parallel normal faults with predominantly NNE-SSW trend forming a number of horsts and grabens within the rift (Minissale et al, 2017).

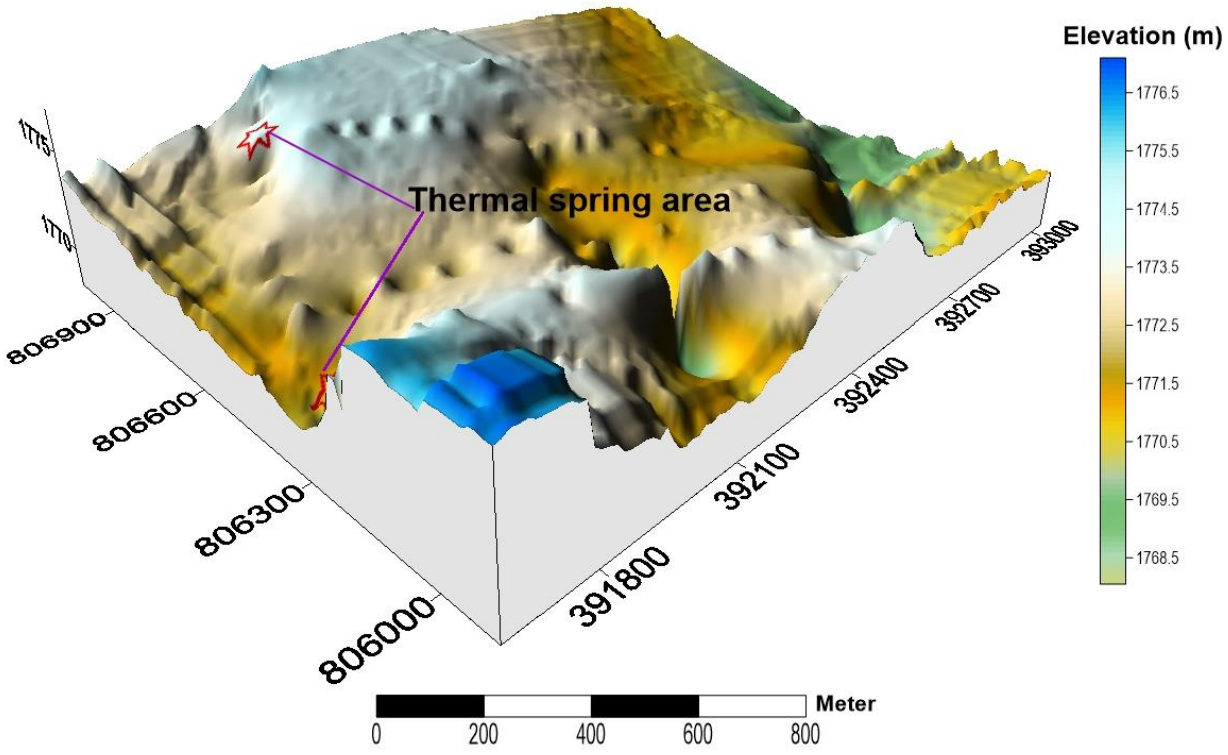

Figure 1.4 Physiography of the study area

The climate of the Alaba is under the Weina Dega weathered condition. The annual rainfall ranges from 857 to 1085 mm, while the annual mean temperature also from 17 °C to 20 °C with a mean value of temperature 18 °C (Figure 1.5).

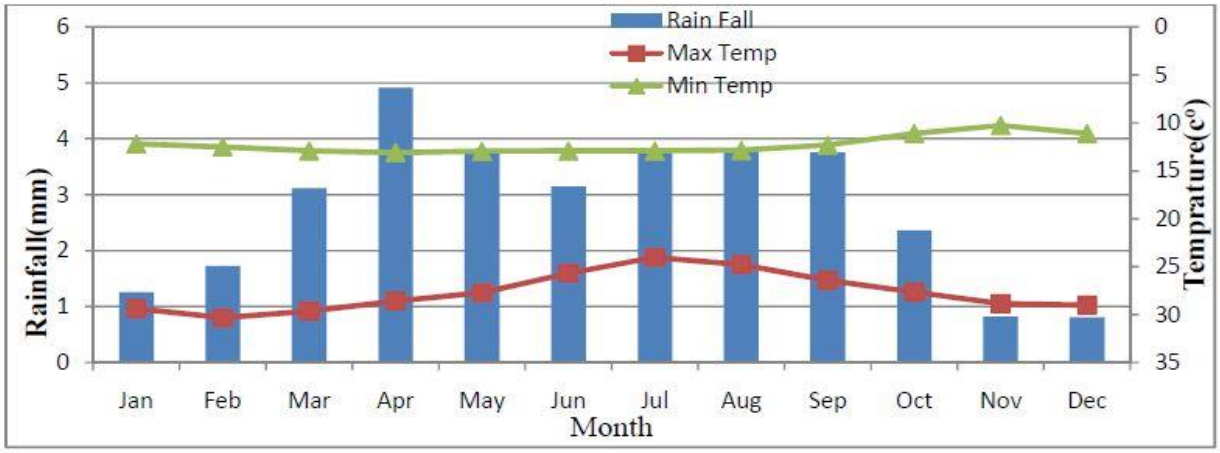

Figure 1.5 Mean monthly rainfall and temperature distribution at Alaba Kulito (1989-2007)

1.3.1 Drainage

In the study area there are a number of springs, some of which are perennial while some dry up in the winter season and reemerge in the summer season. The perennial river in the study area is Bilate river and it flows from Gurage Mt to the Lake Abaya. The spring in the study area flows from the highland of Mt. Dato to the plateau area. The drainage pattern in the Bilate river catchment is characterized by the dendritic pattern.

1.4 Previous works

A large number of publications on the geology, volcano-tectonic, hydrogeology and some on geophysical studies of the Main Ethiopian Rift in general, on the central sector and southern sector in particular, have been produced in the past (UNDP,1973; Tadiwos Chernet, 2011; Minissale et al, 2017).

Geothermal exploration work in the Main Ethiopian Rift and Afar depression was carried out by the United Nations Project of the Ethiopian Institute of Geological Surveys (EIGS-UN) technical team (UNDP, 1973). This reconnaissance study, which included geological, geochemical and geophysical survey, was conducted in a broader area covering the whole Ethiopian Rift Valley. Ethiopia had deep exploration drilling conducted in the Aluto- Langano geothermal field in the

early to mid-1980s. Detailed geological, geochemical and geophysical surveys were carried out over the geothermal field and in the Aluto volcanic center (Berhanu Gizaw, 2008).

Tamiru Alemayehu and Tigistu Haile (2008) studied the Boku thermal area and, is characterized by deep running faults. They suggest that the thermal reservoir is probably receives recharge from multiple sources, but mainly from the regional groundwater system. They conclude main conduits for the thermal recharge from deep-seated thermal sources are probably the Quaternary faults and fractures.

Subsequent studies to evaluate the geothermal resource within the broader lakes district of the MER have indicated that convective hot water systems are contained beneath the Quaternary Rift floor sediments and volcanic rocks. The reservoir was inferred to be within the upper units of the Tertiary volcanic products (mostly ignimbrites) that are exposed on the eastern escarpments that have been down thrown into the rift floor (Lloyd, 1977). It is also widely accepted that Quaternary tectonic movements along the axis of the rift created wide spread secondary permeability and faulted the cap rock whereby a supply of hydrothermal fluid to surface manifestations is maintained.

1.5 Statement of the problem

The study area is located in the Main Ethiopian Rift on the Alaba area (Figure 1.3). The Main Ethiopian Rift has been studied a lot interims of its volcanism and tectonism. Currently, the geothermal resource in the Ethiopian rift is being extensively studied. Many of the geothermal prospect sites have been leased to private companies or joint ventures. The result of these studies are expected to lead towards power generation from these resources. Recently, the studies have increased from time to time to explore the many geothermal potential fields and thermal manifestation areas. In the different geothermal fields of the MER like Aluto- Langano geothermal field a detailed study of hydrothermal alteration, water-rock interaction process (Brhanu Gizaw, 1985, Meseret Teklemariam, 1996), Structural controls on fluid pathways (Hutchison et al., 2015) and detailed characteristics of the geothermal resource is conducted.

Arto hot spring is a wonderful hot spring with an average temperature around 70°C -94°C; quite high temperatures even when compared to many thermal springs of the Ethiopian Rift. The

discharge volume of the spring is also high. The total area of the flat lying grazing land which is inundated during the rainy seasons and turns into a swamp, and over which a stream discharges from the resulting pond created by the spring is about 60sq. meters. Even if there exist a good volume of study conducted on the many hot springs of the Ethiopian Rift, there is limited survey conducted on the Arto hot spring. So in this research is directed at applying geophysical method to acquire information and recognize the Arto hot spring for further detailed investigation and potential use for power generation or other uses like recreational, and thermal healing.

Different researchers including (UNDP, 1973; Tadiwos Chernet, 2011; Minissale et al, 2017) studied the Southern Main Ethiopian Rift geothermal sites. Some of the geothermal sites were studied in terms of geology, geochemistry and understanding of the geothermal system. However, the Arto hot spring was not studied in either one or all of these characteristics like in terms of occurrence, geology, tectonic structure and settings of source the hot spring. This research work will fill this gap by applying two of the most widely used geophysical techniques, i.e. magnetic and electrical resistivity methods which are expected to give additional input towards better understanding of the prospect.

Accordingly, the main goal of this research is to investigate the area with thermal manifestation in the form of hot spring in the Alaba Woreda, specifically the Arto thermal spring area and with a view to understanding their source, reservoir and cap rock. To achieve these goals in this research work, integrated geophysical methods mentioned above would be employed to characterize the thermal setting of the area, understand the role the active tectonic lineaments (faults and fractures) of the Rift play on the hydrothermal springs around Arto.

1.6 Research Question

The research questions is necessitated to identifying the research problem are formulated as follows:

- Which kind of the lithology have been the probable heat source, reservoir and capping rock?
- What is the relationship of the local geological structures in the area with Main Ethiopian Rift structures?

- How the geological structures in the area have been related to thermal manifestation sites?
- What are the major controlling factors for the existence of the Arto geothermal system?

1.7 Objectives of the study

1.7.1 General Objective

The main objective of this research is the geothermal potential assessment of the Arto hot spring by applying integrated geophysical methods.

1.7.2 Specific objective

To achieve this general objective of the research, integrated geophysical techniques will be applied to address the following specific problems:

- To map the subsurface lithology in the close vicinity of the thermal springs.
- To map geological structures (faults, fractures, fissures, contacts, and weak zones) that could play a role in the movement of geothermal fluids
- To determine lateral and vertical extent of the active hydrothermal zones and possible shallow heat sources.
- To examine the potential of the thermal springs for further development and delineate prospective areas for utilization of the thermal springs from surface, near surface and shallow depth source.

1.8 Methodology and material

1.8.1 Methodology

Selecting the appropriate research methodology is the core for solving the problem statement, gain qualified result, and intern the appropriate method is selected based on statement of problem.

Geothermal resource can be explored by using different methods such as geological, geophysical, geochemical and remote sensing. From these methods, geophysical methods are the common one when used with interconnection to the other method used to explore geothermal resource.

To achieve the general and specific objectives of this research, magnetic and electrical resistivity methods were used. Magnetic method is important for geothermal exploration by providing information about the relationship of geothermal activity, the tectonic setting and stratigraphy of the area by means of mapping the anomalies associated with the geothermal system and interpretation of the subsurface geological setting and presence of structures that are essential for the interaction of the geothermal heat, rock and fluid system. The components of the geothermal system, i.e., the heat source, the reservoir and the fluid system, are vital to identify the potential thermal manifestation area. One such useful method is the magnetic method that relies on measuring the variations in the magnetic properties of the rocks in the area (Rivas, 2009).

Electrical Resistivity methods, on the other hand, have been very successfully used in geothermal exploration to identify subsurface anomalies resulting from the geothermal system. The application of electrical resistivity method for geothermal resource exploration has been proved to be productive because of the direct relationship between the presence of fluid and rock temperatures to resistivity.

The activities that are carried out in this research will include literature review, collection of primary data (magnetic and electrical resistivity data) and field observation on the selected geological and structural features. Collection of secondary data like geological map and topo map of the study area is also included in the literature review phase. The primary data collected during fieldwork are to be processed and re-processed using different software packages. The applicable software that are used in this research includes; Geo-Soft, Arc GIS, Surfer, Global Mapper, Google Earth, AutoCAD, IP2win and Win-Resist. Then the results of the data analyzed thus are presented in the form of geophysical anomaly maps and profile plots (for the magnetic data), pseudo depth and geoelectric sections as well as slice and slice-stack plots (for the electrical data). Finally, the results have been qualitatively and quantitatively interpreted. The flow chart shown in Figure 1.6 gives the general flow of the different phases of the works done.

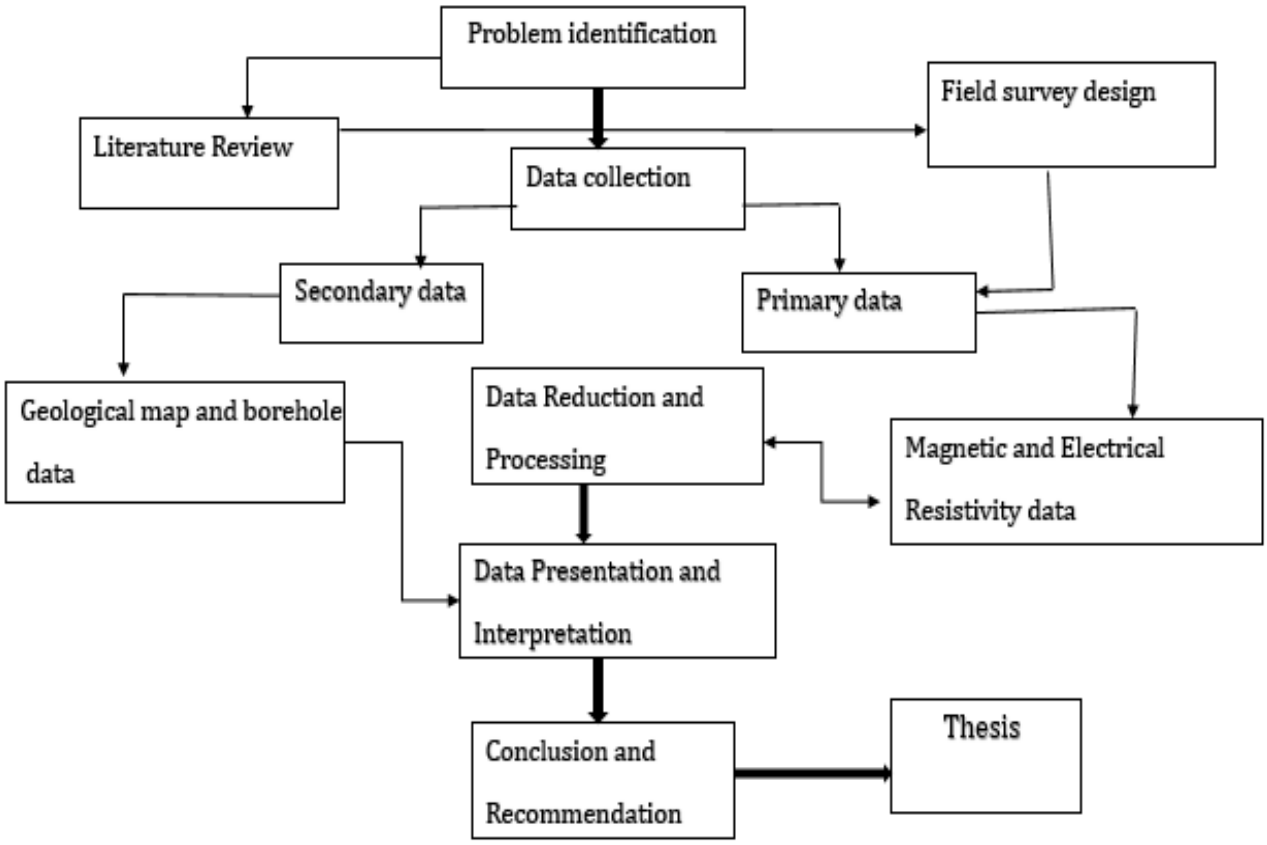

Figure 1.6 Flow chart of the study

1.8.2 Materials

In the research work, once the problem is formulated, identifying the available background material and determining the data gaps, acquiring secondary and primary data, merging of the data set, analysis and presentation of the data and interpretation of the results are the steps one needs to follow in order to solve the problem. A number of material are required to accomplish these and the following material and software are basically used for this thesis work:

- Topographic map with a scale of 1:50,000 from Ethiopian Mapping Agency
- Geological maps are used to know subsurface lithological and structural features
- Google Earth online to help in the assessment of the dominant topographic features of the area before going to the field
- Proton precession magnetometer for magnetic data collection

- PASI 16 GL Earth Resistivity Meter and associated accessories to collect electrical resistivity data
- Global positioning system (GPS) to record the exact data location points
- Arc GIS 10.3 for the preparation of location map of the study area
- Geo-soft for processing, presenting and interpreting of magnetic data
- Win-Resist software to interpret the electrical sounding data processing and Surfer and AutoCAD software to present the data in interpretable form.

1.9 Research outcomes and significance

The expected outcome of study will be

- ✓ Delineating the geothermal potential field in the Arto hot spring area and obtain geophysical data for understanding of the hot spring and establish basic data set for further detailed investigation of the prospect,
- ✓ Knowing the mechanism for the source, reservoir, transporting fluid (possible recharge) and cap rock (if found at shallow depth) of the existing hot spring as starting material for geothermal potential assessment of the Arto thermal springs.

The significance of the research work can be;

- To get a general understanding of the hot spring and suggest its use for small scale recreational and thermal healing purpose for Alaba town and adjoining areas,
- The study will be used as a preliminary study material to plan further exploration phases such as detailed geological, geochemical and geophysical studies.
- The study will also serve as background documented information and as a guidance in a specific subject matter for the concerned bodies like local administration bodies for various purposes.

1.10 Structure of the thesis

This thesis is organized in six chapters. The first chapter is about general introduction of the study area that includes description of study area, objective of the research, methodology used, and statement of the problem and review of previous works. The second chapter is concerned with geology and tectonic setting of the MER, geology and tectonics of the area and hydrogeology of study area.

The third chapter discusses the theoretical background of the geophysical methods of investigation employed in the work compiled from different sources. This chapter explains that briefly the general principles of the methods, instrumentations and data reduction processes followed in both electrical resistivity and magnetic methods of prospecting. Chapter Four states discusses that the data acquisition and presentation schemes which consists of instrumentation, types of array and data acquisition and reduction, processing and presentation of the VES and magnetic data. Chapter five deals with the discussions and interpretation of the processed and presented results of the data or results. The last chapter deals with the conclusions and recommendations of the study based up on the result.

CHAPTER TWO

2 GEOLOGY AND TECTONIC SETTING

2.1 Geology and tectonic setting of the Main Ethiopian Rift

The Main Ethiopian Rift (MER) is a key sector of the East African Rift System (EARS) that connects the Afar depression, at Red Sea-Gulf of Aden junction, with the Turkana depression and Kenya Rift to the South (Corti et al., 2008). The MER is centrally located on the crest of the broad up lift of the Ethiopian dome, between the western plateaus (Abera Alemu, 1992). The MER divided geographically into three sectors: northern, central and southern MER (Corti, 2009; GideyWolde Gabriel et al., 1990; Bonini et al., 2005) characterized by the occurrence of a typical bimodal magmatic activity and two distinct systems of extensional structures (Corti, 2009) a shown given (Figure 2.1) the geological map of CMER. According to Gidey Wolde Gabrieal et al. (1990), the Main Ethiopian Rift divides the 1,000-km-wide uplifted Ethiopian volcanic province asymmetrically into the northwest and southeast plateaus. Volcanic sequences that cover an area several hundred kilometers across are more voluminous and widespread on the northwest plateau than on the opposite side and hence the asymmetry.

The Main Ethiopian Rift, like the rest of the EARS, has undergone a very complicated geological evolution and tectonic history (Mahatsente et al., 1999). The major fault lines in the Main Ethiopian Rift, which are aligned in a NE-SW direction in the Rift floor, form numerous local graven and horst structures (rift-in-rift structures) (Tamiru Abiye and Tigistu Haile, 2008). Its geometry is characterized by normal step faults and well – developed Quaternary faulting that are mostly related to the Wonji Fault Belt (WFB) system of faults with orientation ranging from NNE – SSW to NE-SW (Mohr, 1967 and Boccaletti et al., 1998). The oldest volcanic rocks is the plateau Trap Series, exposed in the western escarpment and consist of basaltic lava with interbedded ignimbrite beds, overlain by massive rhyolites and intervening tuffs and basalts (Merla et al., 1979; Woldegebriel et al., 1990).

The Central Main Ethiopian Rift (CMER) marks the transition between rifting of thick continental crust in the southern and central East Africa Rift System and incipient seafloor spreading in northern Afar. Recent volcanic and tectonic activity in the CMER generally confined to distinct faults belts (Mohr, 1962, 1967; WoldeGabriel et al., 1990).

Most of the recent (Quaternary) volcanic activity in the MER is closely associated with the Wonji faults, as suggested by alignments of caldera structures, cinder cones and volcanic fissures. Geophysical surveys in the Northern MER have shown the presence of magma throughout the lithosphere below the different fault segments, so that the WFB segments represent tectono-magmatic (or magmatic) segments within the central rift valley (Ebinger and Casey, 2001). According to Wolde Gabriel et al. (1990) most of the geological sections exposed along the rift margins are dominated by tertiary volcanic rocks except for a few locations where crystalline basement rocks unconformable overlain by Mesozoic marine sedimentary and/or Tertiary volcanic rocks exist.

The Main Ethiopian rift (MER) is divided in to two in terms of the fault system. These are eastern margin and western margin rift floor (Boccaletti et al., 1998). The western margin of the Main Ethiopian Rift shows a change in fault trend at about 7°5´N. North of this latitude, the margin is well represented by the N35°E-N40°E-trending and ENE dipping high-angle (>60°) Guraghe fault, while to the south the margin is marked by N-S to N20°E striking faults. The eastern margin of the MER, on the other hand, is characterized by high-angle W-dipping N30°E-N40°E-trending border faults, which separate the MER from the Southwestern Plateau. The fault system is articulated and segmented but the overall direction strikes about NE-SW (Boccaletti et al., 1998).

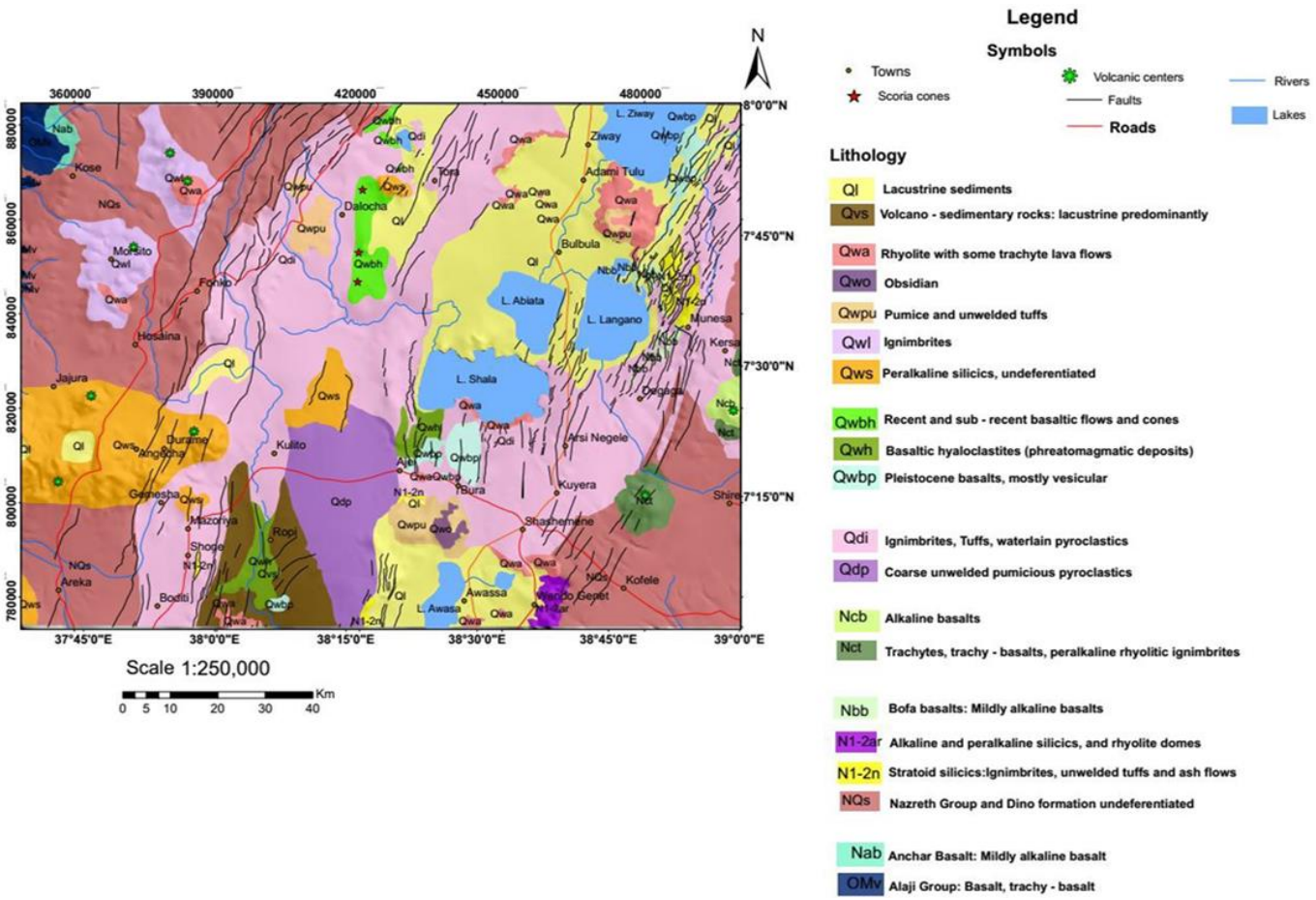

Figure 2.1 Geological map of the Central MER and adjacent plateaus (EIGS, 2012)

2.2 Geology and tectonic setting of the study area

The general geologic set up of the study area and its surrounding is located in the Main Ethiopian Rift floor, is shown in (Figure 2.2).

According to Basalfew Zenebe et al. (2012), the study area is geologically characterized by Dino formation. This formation is not only confined to the rift floor but is extensively developed in escarpments and on the adjacent plateau. The Dino formations are associated with unwelded pyroclastic rocks mainly tuff, ash, ignimbrite, pumice and pyroclastic with occasional intercalated lacustrine beds. This formation is widely exposed at quarry sites and at Bilate riverbed of Shashogo and Alaba special Woreda.

According to Tesfaye Tessema (2015), the eastern part of Alaba town is mostly characterized by acidic volcanic rocks. In the northern direction Alaba Woreda and is geologically covered by pumice and obsidians. The faults in the escarpment areas, which comprises of the older

undifferentiated rocks of Nazret Group and Dino Formation down faulted towards the rift floor resulted in the development of Boyo plain, which is graben.

Volcanic rocks exposed along the southeastern part of the area around Alaba town comprises of enormous accumulation of pyroclastic products of pumice, ash and obsidian. These formations have a high permeability related to intergranular porosity. Its hydrogeological significance is limited because of its area extent and geomorphologic position (Bitsiet Dereje and Dessie Nedaw, 2019).

In the study area, the geological structure are observed in the NE-SW direction, which is with the structures of MER.

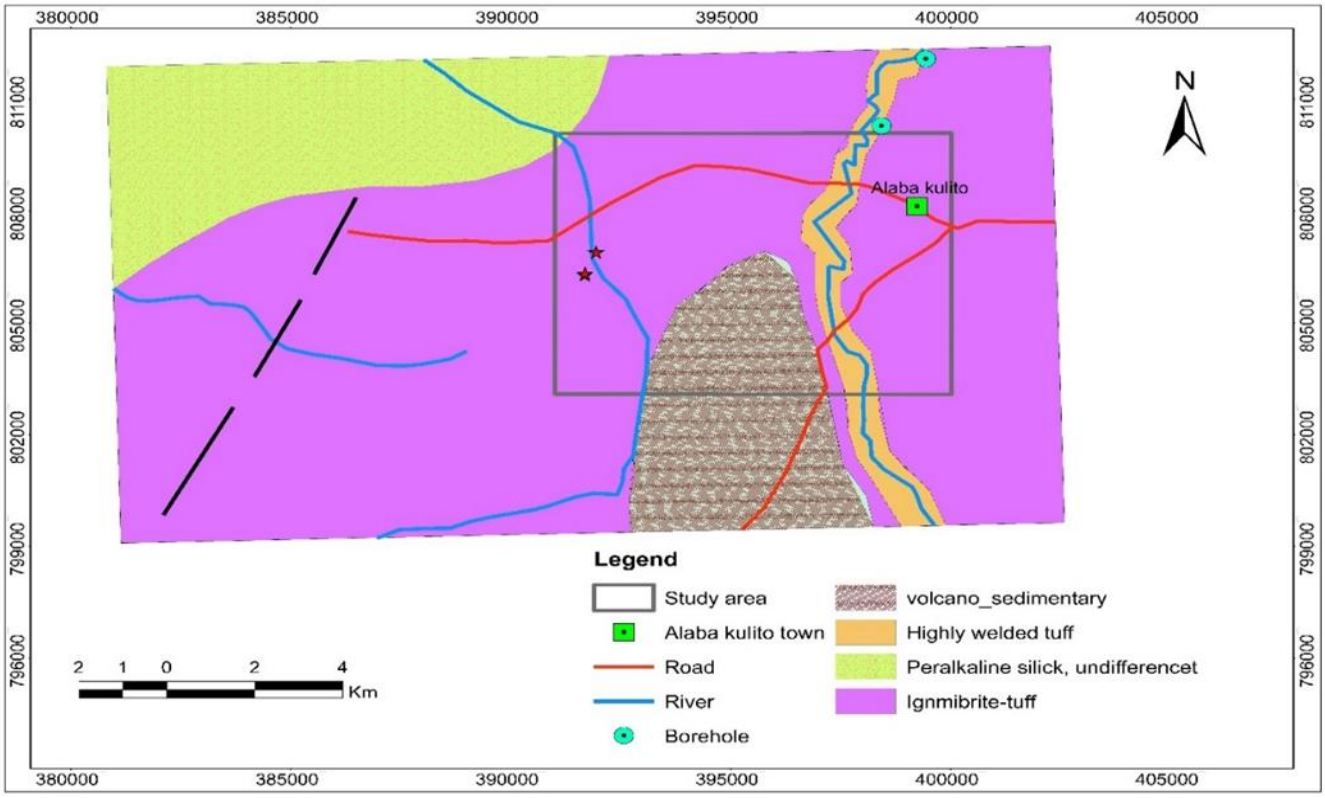

Figure 2.2 Geological map of study area digitized from Hosaina geological map (after Basalfew Zenebe et al., 2012)

2.2.1 Pyroclastic rocks

Pyroclastic rock is the main lithological unit that enormously cover the study area. This unit comprises of pyroclastic products of ignimbrite, pumice and volcanic ash. The ash lithology is

the youngest rock in the study area. The thickness of this lithology is approximately 5m. There is also the ash intercalated with pumice.

The ignimbrite unit are weathered and fractured; the local people use this rock for construction purpose. It is exposed on the Bilate river gorge and is found beneath the ash and pumice. This formation has a high permeability related to intergranular porosity. Its hydrogeological significance is also limited because of its areal extent and geomorphologic position. The fiami has dark color and the rest fine grained and visible crystal. The ignimbrite rock in the study area may be used for geothermal reservoir.

2.2.2 Highly welded tuff

This rock unit is exposed along the Bilate river gorge and the exposure continuing along the Bilate River. This lithological unit is mapped in the Hosaina – Asela geological map sheet.

2.2.3 Volcano-sedimentary rocks

This rock unit is the intercalation of lacustrine sediments with volcanic rocks mainly ashes and tuffs, which in places are extensively developed and the composition is known as volcano sedimentary (Kazmin et al., 1980). The source of this rock is colluvial and outwash debris of along the foothills of the Mt.Dato (Sintayehu Legess, 2009) and Bilate river.

2.3 Hydrogeology of the area

The study area is found in the Bilate river catchment, which have been different tributary to recharge the river, in the eastern direction of the catchment. The occurrence of groundwater in general depends on the geological formation and the subsurface of structure. In the area, the spring which arise from the Mt. Dato highlands and connect to the Bilate river.

According to Sintayehu Legesse (2009), the study area is characterized by volcanic aquifer system, which have been characterized by deep groundwater flow due to the Ambericho fault near Boyo pain and moderate groundwater potential.

Ethiopia has area of complex geology and tectonic features that has strong influence on the emergence of springs. The deep running normal fault to transport either thermally heated or cold

ground water to the surface. The Rift is a thermally rich area due to intensive central volcanic activity and tectonic disturbance since Miocene (Tamiru Alemayehu, 2006).

The Dino – Formation, which forms horst just immediately next to Boyo graben, is less affected by faulting and fracturing. The upper most part is covered with weathered tuff and in some places such as Alaba and Sankura area with thick ash fall deposits. Depth to the groundwater is deeper than the rest of the area (≥200 m). Water is highly mineralized due to long water-rock interaction and the resistivity value is very low. The precipitation of the area is minimal as compared to the west and northern part of the area; this means direct recharge to the groundwater is very low. According to Sintayehu Legesse (2009), the aquifer system of Alaba area is low productive aquifer zone. Eastern part of Alaba area low groundwater potential in high depth has been observed due to very thick pyroclastic acidic rocks especially highly permeable pumice layer that don't retain water at shallow depths but simply allow percolation of recharging water to great depth (Tesfaye Tessema,2015).

The thermal springs, which are associated with the active MER and aligned parallel to it have very high TDS and highly mineralized. The typical examples are Arto thermal spring, which is very close to the southern boundary, Mololicho thermal spring (Sintayehu Legess, 2009). The water flow from high land to the low land therefore it flow from Mt. Amberchio to the Alaba low land and then interconnect with the Bilate river.

CHAPTER THREE

3 THEORETICAL BACK GROUND OF THE GEOPHYSICAL METHODS

3.1 Introduction

Geophysical methods respond to the physical properties of subsurface materials (rocks, sediments, water, voids, etc.), and are divided into two distinct types. Passive geophysical methods detect variations due to natural fields of the Earth, such as the gravitational, magnetic and self/spontaneous-potential field. In contrast, active methods detect Earth's response to artificially generated fields and measure parameters such as electrical resistivity and seismic velocity in which artificially generated signals are transmitted into the ground and detect characteristics of the Earth material. The geophysical instruments measure the signals that are received from the Earth's materials. Then, the output can be displayed and ultimately interpreted.

3.2 Electrical Methods

3.2.1 Introduction

Electrical methods are the most important geophysical methods in the surface exploration of geothermal areas, especially, in delineating geothermal resources and production fields. The electrical resistivity of the rocks, for example, well correlates with the temperature, and alteration of the rocks that are key characteristics for the understanding of the geothermal systems.

In the resistivity method, artificially generated electric currents are introduced into the ground and the resulting potential differences are measured at the surface. This resulted potential difference is characterized the electrical properties of the subsurface.

3.2.2 Principle of the electrical methods

The resistivity method is based on the response of the Earth to the flow of electric current. The working principle of electrical method is that electric current passes into the ground surface by two current electrodes and the second couple of electrodes measure the potential difference. The basic relationship of resistivity and field strength stated in Ohm's law is,

$$E = \rho \vec{J} \tag{3.1}$$

where ***E*** is the electrical field strength (V/m);

J is the current density (A/m^2); and

ρ is the electrical resistivity (Sm), which is a material constant.

The relationship for resistivity and current is:

$$\rho = \frac{V}{I} \tag{3.2}$$

The flow of current in a medium is based on the principle of conservation of charge and is expressed as;

$$div\,\vec{J} = \frac{\partial \rho}{\partial t} \tag{3.3}$$

where ***J*** is the current density (A/m^2) and ρ is the charge density (C/m^2). This relation also known as the equation of continuity. For stationary current this relation is reduced to,

$$div\,\vec{J} = 0 \tag{3.4}$$

The current density **J** is related to the electric field intensity **E** (V/m) as

$$\vec{J} = \frac{1}{\rho}\vec{E} = -\frac{1}{\rho}\,grad\,V \tag{3.5}$$

where ***V*** is the electric potential (volts) and ρ is the resistivity (Ohm-m) of the medium

For an isotropic medium,

$$\text{div}\,[\tfrac{1}{\rho}\text{grad V}] = 0 \tag{3.6}$$

i.e.

$$grad\left(\frac{1}{\rho}\right).grad\,V + \frac{1}{\rho}\,div\,grad\,V = 0 \tag{3.7}$$

This is the fundamental equation of electrical prospecting with direct current If the medium is homogeneous, ρ is independent of the coordinate axes and the relation will be

$$\nabla^2 V = 0 \tag{3.8}$$

which is the Laplace's Equation

3.2.3 Potential due to a point source of current

Let an electrode of small dimension be buried in a homogenous isotropic medium. The current circuit is completed through another electrode, usually placed on the surface, but in any case far enough that its influence at this set up is negligible.

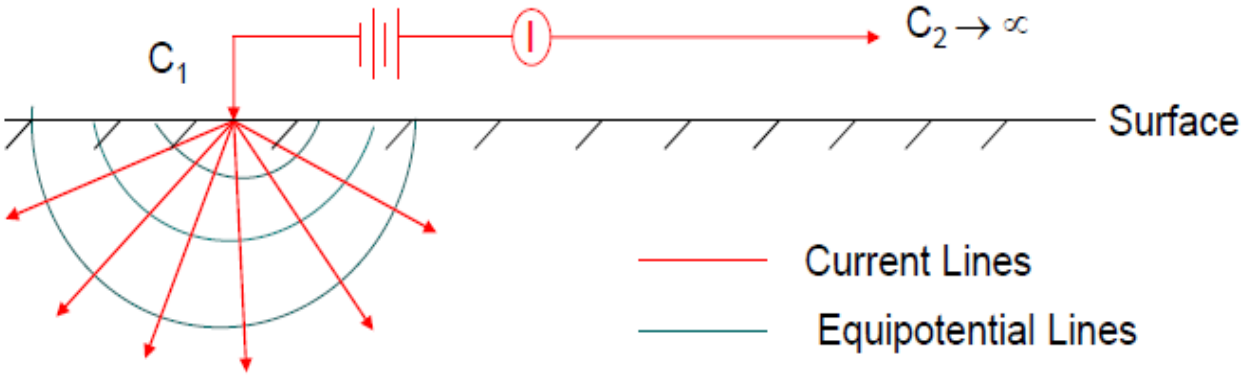

Figure 3.1 Potential due to a point source of current

The determination of the potential at any point P at the surface of an infinite homogeneous medium of resistivity ,ρ due to a point source of current I is the basis for the determination of potential distribution in a layered earth. Under this condition, The Laplace's equation in spherical polar coordinates is most appropriate,

$$\frac{1}{r^2}\frac{\partial}{\partial r}\left(r^2\frac{\partial V}{\partial r}\right)+\frac{1}{r^2\sin\theta}\frac{\partial}{\partial\theta}\left(\sin\theta\frac{\partial V}{\partial r}\right)+\frac{1}{r^2 sin^2\theta}\frac{\partial^2 V}{\partial \emptyset^2}=0 \tag{3.9}$$

For dependence only on ‘r’ this expression reduces to

$$\nabla^2 V = \frac{d^2V}{dr^2} + \frac{2}{r}\frac{dv}{dr} = 0 \quad (3.10)$$

Multiplying throughout by r^2

$$r^2 \frac{d^2V}{dr^2} + 2r\frac{dV}{dr} = 0 \quad (3.11)$$

Integrating both sides of this equation gives

$$\frac{dV}{dr} = \frac{A}{r^2} \quad (3.12)$$

Integrating again

$$V = -\frac{A}{r} + B \quad (3.13)$$

where A and B are integration constants

Boundary Conditions

1. Since V = 0 as r → ∞

B = 0

2. The current flows radially outwards in all directions from the point electrode.

Thus, the total current crossing a spherical surface of radius 'r' is given by

$$I = 4\pi r^2 J$$

$$J = \sigma E, \quad E = -\frac{dV}{dr}, \; \rho = \frac{1}{\sigma}$$

$$I = -4\pi r^2 \sigma \frac{dV}{dr} \quad (3.14)$$

From equation (3.13) and (3.14)

$$I = -4\pi\sigma A$$

Or

$$A = -\frac{I\rho}{4\pi} \quad (3.15)$$

where ρ is the resistivity. Hence, the potential ***V*** is obtained as

$$V = \frac{I\rho}{4\pi} \text{ or } \rho = 4\pi r\left(\frac{V}{I}\right) \quad (3.16)$$

The equipotential which are everywhere orthogonal to the current lines will be spherical surfaces given by V = const.

To measure the potential for the single point is difficult so other way used.

3.2.4 Potential difference when there are two electrodes at the surface

The arrangement of current and potential electrodes and the distances between are as shown in figure 3.1.

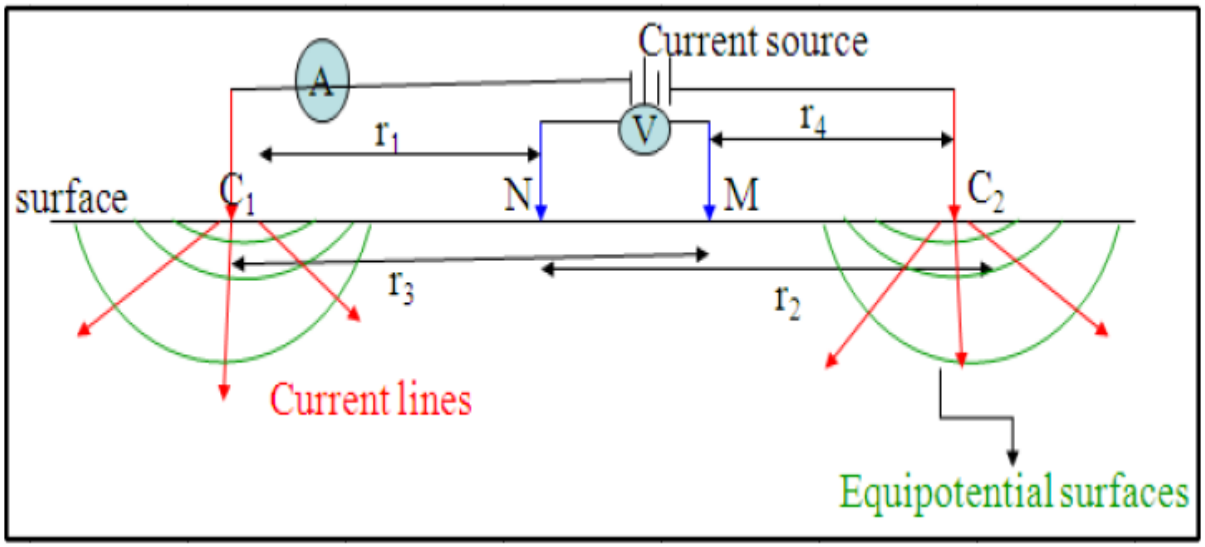

Figure 3.2 The arrangement of current and potential electrode in four-electrode system

The potentaila at P_1, $\mathrm{Vp1} = \frac{\mathrm{I}\rho}{2\pi}[\frac{1}{\mathrm{r1}} - \frac{1}{\mathrm{r2}}]$

Similarly the potential at P_2, $Vp2 = \frac{I\rho}{2\pi}[\frac{1}{r3} - \frac{1}{r4}]$

The potential difference

$$\Delta V = Vp1 - Vp2 = \frac{I\rho}{2\pi}\left[\frac{1}{r1} - \frac{1}{r2} - \frac{1}{r3} + \frac{1}{r4}\right] \quad (3.17)$$

After arranging the distances between the current and potential electrodes according to the well known configurations one can determine the resistivity of the (homogeneous) ground.

3.2.5 Resistivity of rocks

Electrical resistivity of rocks in geothermal surroundings is a parameter, which reflects the properties of the geothermal system, or its history. Thus, a good knowledge on the resistivity of rocks involved is very valuable for the understanding of the geothermal system. This relates to the fact that the resistivity of rocks is chiefly controlled by parameters that correlate to the geothermal activity, such as:

- Porosity and pore structure, where distinction is made between:

- intergranular porosity such as in sedimentary rocks,

- fracture porosity, relating to tension, fracturing or cooling of igneous rocks,

-vugular porosity which relates to dissolving of material (limestone) or gas content (in volcanic magma);

- Alteration of the rocks, lining the walls of the pores, often related to as water-rock interaction;
- Salinity of the fluid in the pores;
- Temperature;
- Amount of water, i.e. saturation or steam content; and
- Pressure

Of all the physical properties of rocks and minerals, electrical resistivity shows the greatest variation. Whereas the range in density, elastic wave velocity, and radioactive content is quite small, in magnetic susceptibility it may be as large as 10^5. However, the resistivity of metallic minerals may be as small as $10^{-5}\Omega$-m, while in dry, close-grained rocks, like gabbro it may go as large as $10^7\,\Omega$-m giving the greatest variation spectrum in electrical resistivity value of rocks.

The resistivity of rocks depend on the water content (porosity) of the rocks, the resistivity of the water contained, the clay content of the rocks and the content of constituent metallic minerals of the rocks. In addition, the resistivity of rocks and minerals exhibit the largest ranges of all physical properties. The resistivity of common Earth materials is given in Table 1

Table1: Resistivity of common geological material (taken from Reynolds, 2011)

Material	Nominal resistivity (Ω m)
Sulphides:	
Chalcopyrite	1.2×10^{-5}–3×10^{-1}
Pyrite	2.9×10^{-5}–1.5
Pyrrhotite	7.5×10^{-6}–5×10^{-2}
Galena	3×10^{-5}–3×10^{2}
Sphalerite	1.5×10^{7}
Oxides:	
Hematite	3.5×10^{-3}–10^{7}
Limonite	10^{3}–10^{7}
Magnetite	5×10^{-5}–5.7×10^{3}
Ilmenite	10^{-3}–5×10
Quartz	3×10^{2}–10^{6}
Rock salt	3×10–10^{13}
Anthracite	10^{-3}–2×10^{5}
Lignite	9–2×10^{2}
Granite	3×10^{2}– $\times 10^{6}$
Granite (weathered)	3×10–5×10^{2}
Syenite	10^{2}–10^{6}
Diorite	10^{4}–10^{5}
Gabbro	10^{3}–10^{6}
Basalt	10–1.3×10^{7}
Schists (calcareous and mic	20–10^{4}
Schist (graphite)	10–10^{2}
Slates	6×10^{2}–4×10^{7}
Marble	10^{2}–2.5×10^{8}
Consolidated shales	20–2×10^{3}
Conglomerates	2×10^{3}–10^{4}
Sandstones	1–7.4×10^{8}
Limestones	5×10–10^{7}
Dolomite	3.5×10^{2}–5×10^{3}
Marls	3–7×10
Clays	1–10^{2}
Alluvium and sand	10–8×10^{2}
Moraine	10–5×10^{3}

Material	Nominal resistivity (Ω m)
Sherwood sandstone	100–400
Soil (40% clay)	8
Soil (20% clay)	33
Top soil	250–1700
London clay	4–20
Lias clay	10–15
Boulder clay	15–35
Clay (very dry)	50–150
Mercia mudstone	20–60
Coal measures clay	50
Middle coal measures	> 100
Chalk	50–150
Coke	0.2–8
Gravel (dry)	1400
Gravel (saturated)	100
Quaternary/Recent sands	50–100
Ash	4
Colliery spoil	10–20
Pulverised fuel ash	50–100
Laterite	800–1500
Lateritic soil	120–750
Dry sandy soil	80–1050
Sand clay/clayey sand	30–215
Sand and gravel	30–225
Unsaturated landfill	30–100
Saturated landfill	15–30
Acid peat waters	100
Acid mine waters	20
Rainfall runoff	20–100
Landfill runoff	< 10–50
Glacier ice (temperate)	2×10^{5}–1.2×10^{8}
Glacier ice (polar)	5×10^{4}–3×10^{5} *
Permafrost	10^{3}– > 10^{4}

3.3 Magnetic methods

Magnetic method is geophysical method used to geothermal exploration. This method can be used in geothermal exploration because ferromagnetic minerals will lose their magnetism when heated in high temperature. Magnetic surveys are carried out to map subsurface geology using the variation of the distribution of magnetic minerals. In general, the magnetic content (susceptibility) of rocks is extremely variable depending on the type of rock.

Magnetic and gravity method have much in common, but magnetics more complex and variation in magnetic field are more erratic and localized. This is partly due to the difference between dipolar in magnetics field and the mono polar in gravity field (Telford et al., 1990).

The aim of a magnetic survey is to investigate subsurface geology based on anomalies in the Earth's magnetic field resulting from the magnetic properties of the underlying rocks. Although

most rock-forming minerals are effectively non-magnetic, certain rock types contain sufficient magnetic minerals to produce significant magnetic anomalies. Similarly, man - made ferrous objects also generate magnetic anomalies. Magnetic surveying thus has a broad range of applications, from small-scale engineering or archaeological surveys to detect buried metallic objects, to large-scale surveys carried out to investigate regional geological structure (Kearey et al., 2002).

Magnetic surveys can be performed on land, at sea and in the air. Consequently, the technique is widely employed, and the speed of operation of airborne surveys makes this survey method very attractive in the search for types of ore deposit that contain magnetic minerals. In small-scale local site characterization like mapping of structures, structural discontinuities, and weak zones as well as for detailed investigation of mineralized zones, however, magnetic survey is an indispensable tool.

3.3.1 Principle of the magnetic method

If two magnetic poles of strength P_0 and P_1 are separated by a distance r, a force ($\boldsymbol{F}$) exists between them. When the poles have the same polarity, the force will push the poles apart whereas pole with opposite polarity, possess attraction, and will be drawn together. The equation for the force $\boldsymbol{F}$ is obtained from coulomb's law and is mathematically given by:

$$F = \frac{1}{\mu}\frac{P_0 P_1}{r^2} \tag{3.18}$$

The constant μ, known as magnetic permeability, depend upon the magnetic properties of the medium in which the poles are situated.

The magnetic field $\boldsymbol{B}$ due to a pole of strength P at a distance r from the pole is defined as the force exerted on a unit positive pole at that point

$$B = \frac{\mu o P}{4\pi\mu R r^2} \tag{3.19}$$

Magnetic fields can be defined in terms of magnetic potentials in a similar manner to gravitational fields. For a single pole of strength *P*, the magnetic potential ***V*** at a distance *r* from the pole is given by

$$V = \frac{\mu o\ P}{4\pi\mu R\ r} \tag{3.20}$$

The magnetic field component in any direction is then given by the partial derivative of the potential in that direction. Common magnets exhibit a pair of poles is referred to as dipoles. The magnetic moment ***M*** of a dipole with poles of strength m a distance L apart is given by

$$M = mL \tag{3.21}$$

The magnetic moment of a current-carrying coil is proportional to the number of turns in the coil, its cross sectional area and the magnitude of the current, so that magnetic moment is expressed in Am^2.

When a material is placed in a magnetic field, it may acquire a magnetization in the direction of the field, which is lost when the material is removed from the field. This is phenomenon referred to as induced magnetization or magnetic polarization, and results from the alignment of elementary dipoles within the material in the direction of the field. Because of this alignment, the material has magnetic poles distributed over its surface, which correspond to the ends of the dipoles. The intensity of induced magnetization **Ji** of a material is defined as the dipole moment per unit volume of material:

$$Ji = \frac{M}{LA} \tag{3.22}$$

where ***M*** is the magnetic moment of a sample of length *L* and cross-sectional area *A*. J_i is consequently expressed in Am^{-1}.

The magnetic response of rocks and materials is determined by the amounts and susceptibilities of magnetic materials in them (Telford et al, 1990).The induced intensity of magnetization is proportional to the strength of the magnetizing force ***H*** of the inducing field: i.e

$$Ji = kH \tag{3.23}$$

where '*k'* is the magnetic susceptibility of the material. Since $\boldsymbol{J}_i$ and $\boldsymbol{H}$ are both measured in Am^{-1}, susceptibility is dimension less in the SI system.

Within the body the total magnetic field, or magnetic induction, $\boldsymbol{B}$ is given by

$$B = \mu oH + \mu oJi \tag{3.24}$$

Substituting equation (3.23)

$$B = \mu oH + \mu okH = (1 + k)\mu oH = \mu R\mu oH \tag{3.25}$$

Where μ_R is a dimensionless constant known as the relative magnetic permeability. The magnetic permeability 'm' is thus equal to the product of the relative permeability and the permeability of vacuum, and has the same dimensions as μ_o. For air and water μ_R value is thus close to unity.

3.3.2 The Earth's magnetic field

The Earth's magnetic field consists of three components. These are the main field, the external field (fluctuating field) and magnetized materials within the Earth's crust (local anomaly field).

The main field, which accounts for over 99% of the Earth's total magnetic field, is internal in origin and is thought to be caused by convection currents of conducting material (mainly iron and nickel) within the liquid outer core. The Earth's main magnetic field approximates, to a first degree, the field of a magnetic dipole and is the inducing field for magnetized objects within the earth's crust. The main field consists of several magnetic elements, which are important in understanding the measured magnetic anomaly patterns. These elements include: 1) magnitude of the field (F), 2) magnetic inclination (I) which is the dip of a magnetic compass needle from horizontal (e.g., magnetic south pole is -90° , magnetic north pole is 90°, and magnetic equator is 0°), and 3) magnetic declination (D) which is the angle between geographic and magnetic north. Figure 3.3 shows Earth magnetic field components.

Additionally, the Earth's main magnetic field changes with time due to variations in the motion of the convection currents within the outer core. These long period, slow changes (called westward drift or secular variations) cause the magnitude, inclination and declination to change with time. A mathematical formula derived using magnetic records over the surface of the Earth

in a reverse sense (i.e. knowing the field and determining what mathematical expression best represents the measured field and its variation) is given in what is called the International Geomagnetic Reference Field (IGRF). The IGRF is normally updated every five years or so and is revised to give the DGRF (Definitive), which becomes the prevalent reference model of the Earth's magnetic field for that particular period. The current DGRF can be obtained from the national geophysical data center of the National Oceanic and Atmospheric Agency (NOAA, 2011).

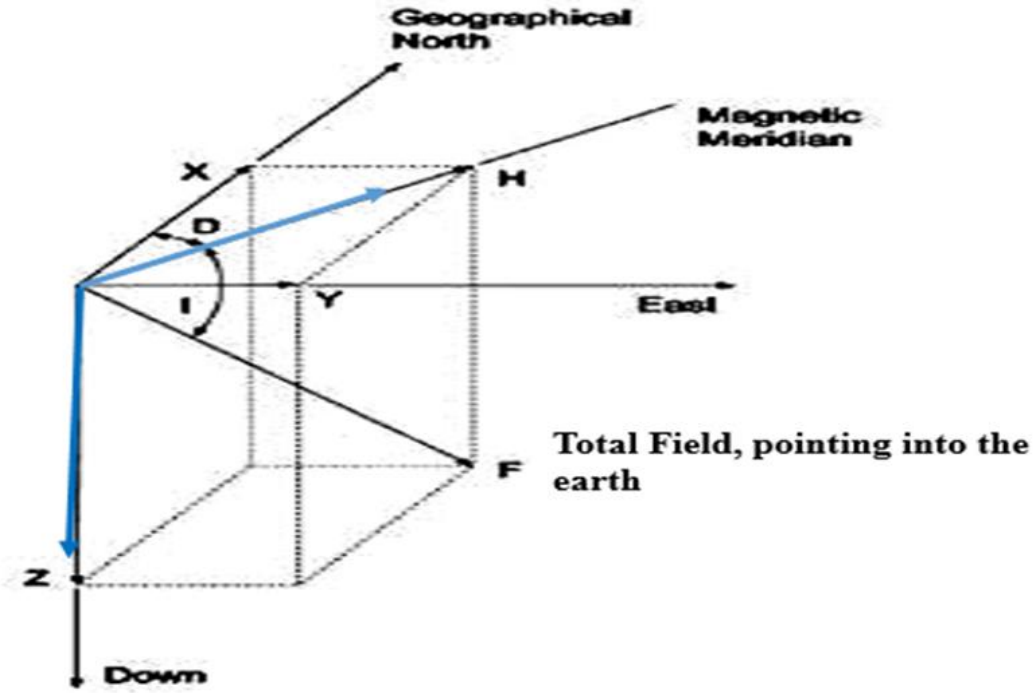

Figure 3.3 Earth magnetic field components

The other part of the Earth's magnetic field, the external magnetic field (also called diurnal field) is due to electric currents within the Earth's ionosphere. These currents are mainly caused by interactions of the main field with plasmas connected with solar winds. These diurnal variations fields fluctuate rapidly but smoothly with time (minutes to hours) with maximum amplitudes varying from 50 to 200 gammas. On some days, these fluctuations are more random with amplitudes of several hundred gammas to give rise to what are called magnetic storms. These storms are associated with solar flares and sunspot activity, and may persist for hours or several

days. During such storms, magnetic surveying should be stopped and change be made to the survey time.

On the other hand, magnetized materials within the Earth's crust create small amplitude magnetic fields that cause spatial variations of the Earth's main magnetic field. The variations in these fields result from spatial variations in subsurface lithology. These materials are the targets of the magnetic method of prospecting.

3.3.3 Magnetic Properties of Earth materials

Different types of magnetic materials are due to differences in their response to external magnetic fields. Some materials are much more magnetic than others .The reason is in some materials there is a strong interaction between the atomic magnets, where as in other materials there is no interaction between the atomic magnets. Depending upon the magnetic behavior of materials, they can be classified as: diamagnetic, paramagnetic, ferro-magnetic, ferri-magnetic and anti-Ferro-magnetic substances.

Magnetic susceptibility is the significant variable in magnetics surveys. It plays the same as density does in gravity interpretation. Although instrument are available for measuring susceptibility in the field, the can only be used on outcrops or on rock samples and such measurements do not necessarily give the bulk susceptibility of the formation.

The susceptibility of a rock usually depend on its magnetic content. Basic igneous rocks are usually highly magnetic due to their relatively high magnetite content. The proportion of magnetite in igneous rocks tends to decrease with increasing acidity so that acid igneous rocks, although variable in their magnetic behavior, are usually less magnetic than basic rocks. Metamorphic rocks are also variable in their magnetic character. Their magnetic character is associated with the generally small proportion of magnetic minerals that they contain (Reynolds, 1997).

The magnetite content and susceptibility of rocks is extremely variable and there can be considerable overlap between different lithology. Itis not usually possible to identify with certainty the causative lithology of any anomaly from magnetic information alone. However, sedimentary rocks are effectively non-magnetic unless they contain a significant amount of

magnetite in the heavy mineral fraction. Where magnetic anomalies are observed over sediment covered areas the anomalies are generally caused by an underlying igneous or metamorphic basement, or by intrusions into the sediments. Table 2 gives the magnetic susceptibility of some Earth materials.

Table 2: Susceptibilities of rocks and minerals in SI units (taken from Reynolds, 2011)

Mineral or rock type	Susceptibility*	Mineral or rock	Susceptibility*
Igneous		*Metamorphic*	
Granite	10 to 65	Schist	315 to 3000
Granite (m)	20 to 50000	Slate	0 to 38000
Rhyolite	250 to 37 700	Gneiss	125 to 25 000
Pegmatite	3000 to 75 000	Serpentenite	3100 to 75 000
Gabbro	800 to 76000	Average for	0 to 73000
Basalts	500 to 182000	*Minerals*	
Oceanic basalts	300 to 36 000	Ice (d)	—9
Pendotite	95 500 to 196000	Rocksalt (d)	-10
Average for acid	40 to 82 000	Gypsum (d)	-13
Average for basic	550 to 122000	Quartz (d)	-15
Sedimentary		Graphite (d)	- 80 to – 200
Dolomite (pure)	-12.5 to + 44	Chalcopyrite	400
Dolomite (impure)	20000	Pyrite (o)	50 to 5000
Limestone	10 to 25 000	Hematite (o)	420 to 38 000
Sandstone	0 to 21 000	Pyrrhotite (o)	1250 to 6.3 x 10^6
Shales	60 to 18 600	Ilmenite (o)	314 000 to 3.8x10^6
Average for various	0 to 360	Magnetite (o)	70000 to 2 x 10^7

(d) = diamagnetic material; (o) = ore; (m) = with magnetic $\kappa \times 10^6$ SI units; to convert to the c.g.s. units, divide by 4π.

It is clear from the table that Earth materials generally show very large variations in magnetic susceptibility and significant overlap, and interpretation of magnetic anomalies interims of particular causative body/bodies is a difficult task. However, interpretation of the variations in terms of variations in lithology and presence of contacts is plausible.

3.3.4 Temporal variations the Earth's magnetic field

The Earth's magnetic field changes its direction and intensity with time. As a result, the temporal variation of the Earth's magnetic field can be explained in terms of three types and causes.

Secular variation: These are very long period changes that result from convective changes in the core. They are controlled by long time measuring changes in inclination, declination and

magnetic field of the Earth's geomagnetic field at observatories. Due to the presence of variation, occur slowly with respect to the time of completion.

Diurnal variations: Magnetic effects of external origin cause the geomagnetic field to vary on a daily basis to produce diurnal variations. In the normal conditions, the diurnal variation is smooth and regular. This variation should be accounted when conducting exploration magnetic surveys.

Magnetic Storms: In addition to the relatively predictable and smoothly varying diurnal variations, there can be transient, large amplitude (up to 1000 nT) variations in the field that are referred to as Magnetic Storms. The frequency of these storms generally correlates with sunspot activity. Based on this, some prediction of magnetic storm activity is possible. The most intense storms can be observed globally and may last for several days. Magnetic surveys are normally interrupted during such events as the magnitude of these variations are quite large as compared to the small magnitude variations resulting from variations in local lithology.

3.3.5 Magnetic surveying

Magnetic exploration can be carried on land, at sea, and in the air. Magnetic surveys either directly seek magnetic bodies or they seek magnetic material associated with an interesting target. Magnetic survey on land are usually done with portable proton precession magnetometers. The Profiles or networks of points are measured in the same way as for gravity. It is important to survey perpendicular to the strike of an elongate body or two-dimensional modeling may be very difficult.

The first stage in any magnetic survey is to check the magnetometers set up including the tuning field i.e. the magnitude of the field over the area to be surveyed. This can be obtained from printed maps of geomagnetic elements from which the field for the area close to the survey site can be picked. The second task will be setting a magnetically clean environment for the magnetometer. Operators can be potent sources of magnetic noise, although the problems are much less acute when sensors are on long poles than when they are carried in backpacks or when, as with fluxgates, they must beheld close to the body. Compasses, pocketknives and geological hammers are all detectable at distances of less than about a meter, and users of high-

sensitivity magnetometers may need to visit tailors (and cobblers) for non-magnetic clothing. Survey vehicles can be detectable at distances of up to 20 m. The safe distance should be determined before starting survey work.

As a next stage, the design of a survey and the procedures used in data acquisition are determined. These are factors including the objectives of the survey, the size, location, and physical characteristics of the study area, the anticipated source sand nature of magnetic anomalies and noise, and the resources available. Magnetic survey then proceeds with establishment of a base station, ideally close to the survey lines (so as reoccupation is not arduous) but magnetically free from the potential target. Survey start by taking reading/s at the base station and then moving on to the measuring stations and return to the base station at regular and as short as possible intervals to take repeat base station readings. The repeat readings from the base station are used for diurnal correction. Repeat readings at the base station that are preferred to be as many number of readings as possible each time it is occupied could also be averaged out to give the main field value over the surveyed area. This provides an alternative way (to that of IGRF values, see section 3.3.6) for removing the main field from the readings-m correction for the secular field. Readings are also to be taken at the base station at the end of the survey so that instrument drift corrections can be effected if required.

3.3.6 Noise and corrections for magnetic variations

All magnetic data sets contain element of noise and will require some form of correction to the raw data to remove all contributions to the observed magnetic field other than those caused by sub-surface magnetic sources. In ground magnetometer surveys, it is always advisable to keep any magnetic objects (keys, penknives, some wristwatches, etc.), which may cause magnetic noise, away from the sensor. It is also essential to keep the sensor away from obviously magnetic objects such as cars, metal sheds, power lines, metal pipes, electrified railway lines, walls made of mafic rocks, etc.

There are several ways of correcting magnetic data according to the various magnetic variations. For the secular variation of magnetic data, a model known as International Geomagnetic Reference Field (IGRF) has been prepared from comparison of individual magnetic responses in different areas of magnetic observatories. Therefore, it has become standard processing practice

for magnetic survey that the applicable IGRF (updated to the time of the survey) for the base station value is subtracted from the observed values of the total magnetic intensity.

The next most significant correction is for the diurnal variation in the Earth's magnetic field. The necessary corrections are mostly attempt by the reoccupation of the base station (section 3.3.5), which is located in or near the survey area. Variations in magnetic field due to magnetic storms can be so rapid, unpredictable, and of such large amplitude, that normally no corrections practical and under such conditions magnetic surveying is normally discontinued.

CHAPTER FOUR

4 DATA ACQUISITION AND PROCESSING

4.1 General

This research work has utilized electrical resistivity and magnetic methods. The data used were primarily collected electrical resistivity and magnetic data. The survey line was selected perpendicular to the discharge of the hot spring direction.

Electrical resistivity is a fundamental property of rocks and is closely associated with their lithology. The direct current method is commonly used for determining the resistivity of subsurface rocks by passing a known current through the ground and measuring the strength of the current flow at the surface. Electrical resistivity method is important for geothermal investigation by identifying the source rock for heat source, the zone of fluid saturation and capping rock. On the other hand.

The magnetic method is a well-known technique to identify subsurface structures and contact between lithological units. Magnetic method is also applicable for geothermal exploration by identifying the structures of subsurface for transport of geothermal fluids.

4.2 Electrical resistivity survey

4.2.1 Instrumentation and data acquisition

The basic equipment required for electrical resistivity survey consists of the resistivity unit that injects current to the ground (transmitter), measures the current strength as well as determine the potentials (receiver) using as double pair of steel electrodes, hammers, electrical cables and

connectors. The instrument used as transmitter and receiver for this survey is the PASI 16GL Earth Resistivity Meter along with P100 energizer DC source.

The Schlumberger array as in most cases was used for vertical electrical sounding for its better depth of penetration The array, however, is less sensitive for lateral inhomogeneity because the potential electrodes remain fixed during a number of successive measurements with expanding current electrodes. Electrical current are injected in to the ground by means of two outer electrodes and the resulting potential difference were measured by a second pair of potential electrodes placed near the center of the outer electrodes. Current electrode separation (AB/2) was progressively increased in the each of measurements in order to acquire data from deeper horizons.

The PASI-16 GL (Figure 4.1) equipment was setup by ensuring the electrodes are well hammered into the ground making a sound galvanic contact and cables were connected to both current and potential electrode terminals.

Figure 4.1 (a) PASI-16 GL and P-100 energizer instrument and (b) during field survey with cables and reels.

For this study, vertical electrical sounding was conducted along three near parallel profile lines. The lines are separated by about 400m for Line 1 and Line 2 whereas the separation is 430m for Line 2 and Line 3. Most of the sounding were carried out with the maximum half current

electrode spacing (AB/2) of 750m. Only in a few cases where the linear clearing does not allow increased separation, AB/2 of 500m were used.

Totally, nine vertical electrical sounding were taken to understand the subsurface of the study area. Each profile line contains three VES. The profile line are nearly parallel and approximately oriented northeast- southwest direction in the area (Figure 4.2). The azimuth of the expanding spread for each VES point is approximately in an E- W direction.

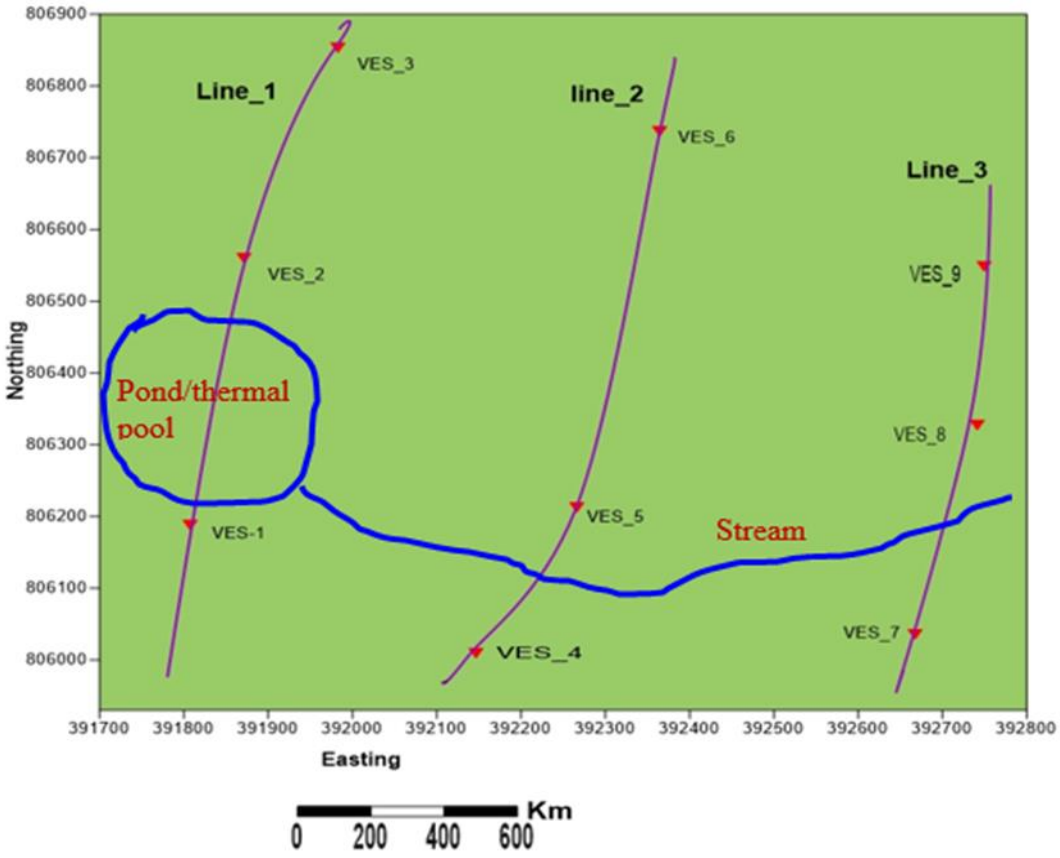

Figure 4.2 Location of VES survey lines and sounding data points

4.2.2 Electrical resistivity data processing

After the field data have been collected, the raw resistivity data were entered to the excel sheet and prepared for different software to be processed. The apparent pseudo depth section along profile and the apparent resistivity sliced pseudo depth section for different current electrode spacing (AB/2) were prepared by Surfer 10 software. The software used for constructing the

geoelectric section- i.e. a plot of the true resistivity verses true depth is the AutoCAD software. The initial layer parameters (resistivity and thickness of the horizons mapped beneath each sounding point) for AutoCAD was obtained by the winResit software.

4.3 Magnetic survey

4.3.1 Instrument and data acquisition

The instrument used for magnetic data collection is Proton Precession Magnetometer-600, show in Figure 4.3. A proton precession magnetometer is one of the most accurate devices that one can build for measuring total magnetic fields. The instrument works through protons rotation, which have an intrinsic magnetic field, it like a small magnet. When the protons are place in an external magnetic field, the direction of their field will precess (rotate) about the direction of the external field.

The proto precession magnetometer depend on the measurement of the free- precession frequency of proton (hydrogen nuclei) that have been polarized in a direction approximately normal to the direction of the Earth magnetic field (Telford et al, 1990). When enough protons are precessing in sync about an external field (the geomagnetic field in this case), they will produce an oscillating magnetic field, due to the combined effect of each of their processing fields. The frequency of this oscillating field is ultimately, what is measured by the proton precession magnetometer and since it is equal to the precession frequency of the protons it can be used to determine the strength of the external field.

Figure 4.3 Magnetic data acquisitions at field using proton precession magnetometer-600

Detailed magnetic survey was conducted over the survey area with as many parallel and cross profile lines as possible employed. During field survey, single proton precession magnetometer was used. The survey was conducted on six-survey line (Figure 4.4) with station spacing of 10m. Three of the survey lines are parallel to the VES profiles while the other three are perpendicular to these. A total of 311 magnetic data points were collected.

Before any measurement was taken, a single base station for all the observations was occupied to be used for correcting the diurnal effect. Field stations were consequently occupied to take station readings. Repeat readings were taken for each field station occupied to ascertain minimum deviation in instrument readings. Accordingly, all the primary magnetic data were collected covering the area of interest as much as possible and were made available for further reduction and processing steps.

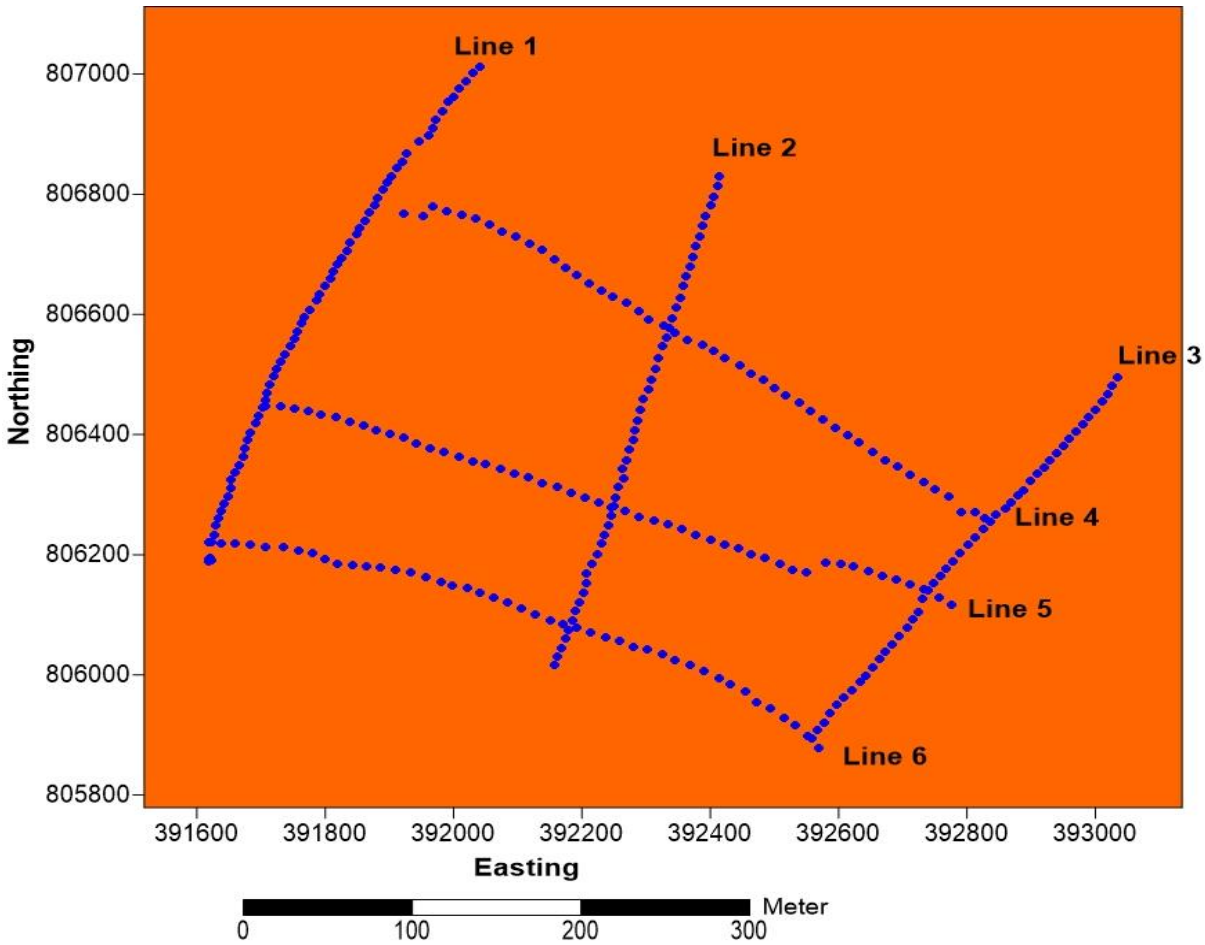

Figure 4.4 Magnetic survey lines and data points

4.3.2 Magnetic data reduction and processing

4.3.2.1 Magnetic data reduction

Magnetic survey was started and ended by taking base station readings while occupying each survey line. For all the survey lines a single common base station was used and this is an advantage because it gives large number of readings to average out and define the predominant total field value over the survey area.

Magnetic data correction is a necessary step to remove the noise from the data that are not related with the effect of the subsurface material. The magnetic noise may be diurnal variation, magnetic storm and main field value that forms the background of the measured fields. These

variations must be corrected for except the magnetic storm to get real subsurface information. Magnetic storm cannot be corrected if it occurs during field survey and usually a change in the time or day for reading of data is the right measure to be taken. For very short period magnetic storms, taking a few minutes of break in data reading until the field returns to the normal value will be adequate. Diurnal correction is done by subtracting the diurnal variation of each magnetic reading point from the corresponding field readings. IGRF correction is by averaging out all the base station readings and subtracting this average value from the total magnetic reading value of each station to determine the anomaly.

4.3.2.2 Magnetic data processing

The corrected magnetic data processed using different filtering technique and the Geosoft Oasis Montaj V.7 Software enhances corrections. The processed map is used for qualitative and quantitative interpretation, which in turn helps to identify the anomalous body.

The total magnetic anomaly values have been used for separating the residual magnetic anomaly and the regional magnetic anomaly. Furthermore, analytical signal, tilt derivative and Euler deconvolution magnetic maps were processed and enhanced from the residual magnetic map by using the Geosoft Oasis Montaj (Version 7.0.1). The entire processed magnetic anomaly are presented in the form of different magnetic anomaly maps and profile.

CHAPTER: FIVE

5 RESULT AND INTERPRETATION

Geophysical data are presented in different forms and interpreted based upon the objectives of the research and the methods used. In data presentation, the output of each geophysical technique employed was used to produce different plots that show the physical property of the subsurface Earth materials. For this study, pseudo depth sections, slice and slice-stacked section were plotted using the raw sounding data and following these the VES data are interpreted interims of layer parameters and the layer parameters thus obtained are used to construct the geo-electrical section from VES data. From the magnetic data; total magnetic field anomaly, residual magnetic anomaly, tilt derivative magnetic anomaly and Euler deconvolution magnetic maps were produced.

5.1 Electrical resistivity result and interpretation

5.1.1 Interpreted VES curve

The Apparent resistivity versus electrode spacing was plotted on the bi-log scale and interpreted using IP2Win to acquire the initial layer parameters (resistivity and depth) of Winresist software. The interpreted VES curves are highly correlate with the electrical field data and the interpreted model with RMS error of 2.8 to 4.6%. Three VES points were sampled from each survey lines shown in Figure 5.1. The other VES curve points were found in the appendix 1.

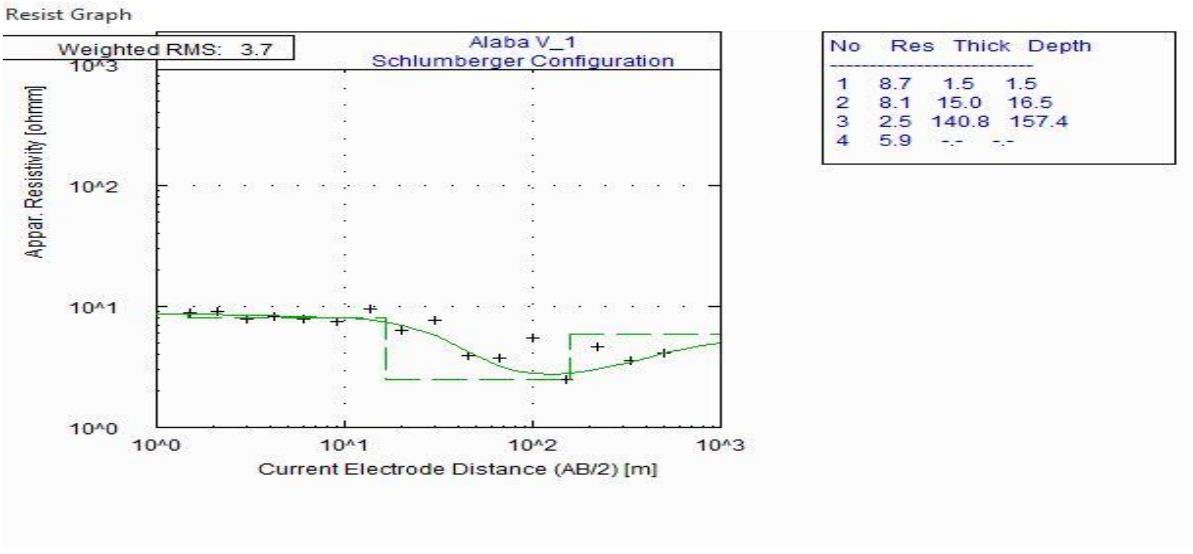

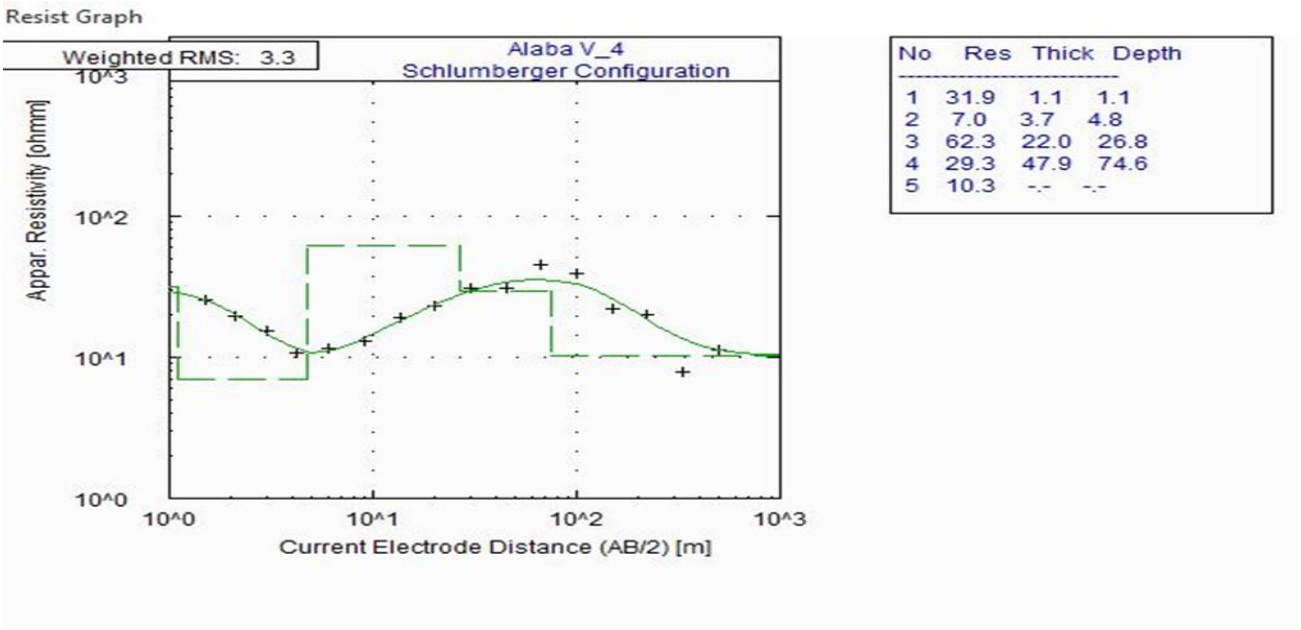

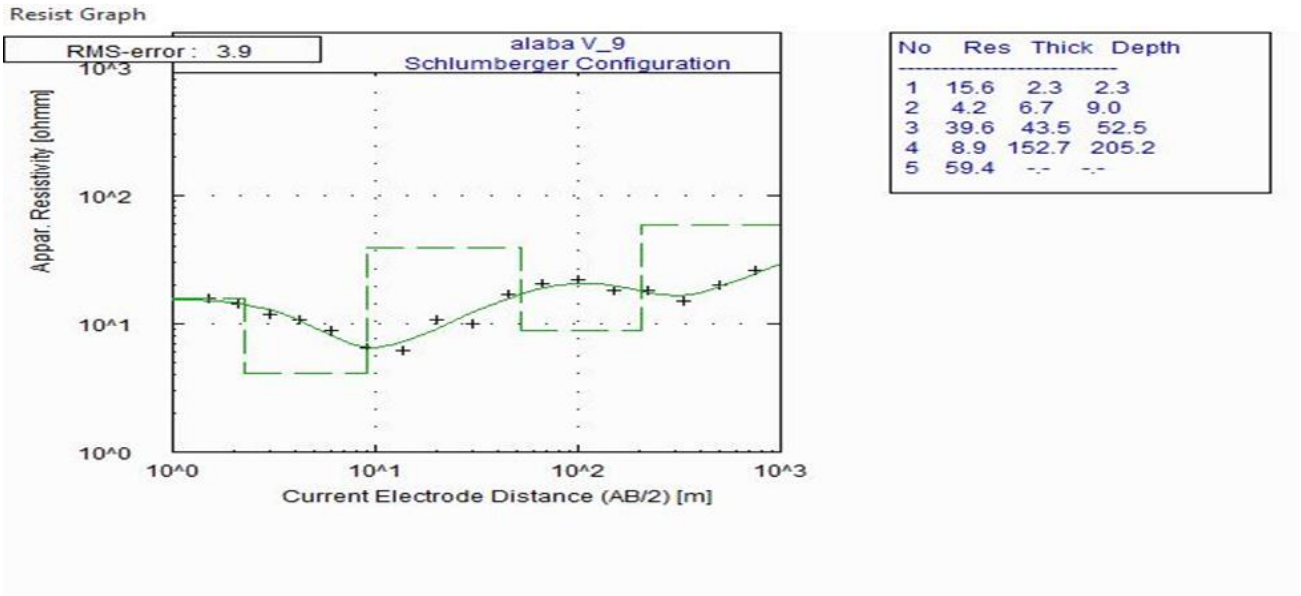

Figure 5.1 Interpreted VES curve

5.1.1 Sliced-Stacked map for various AB/2

The sliced stacked map is visualize the overall distribution of subsurface at laterally and vertically interims of their resistivity.

The sliced stacked map of apparent resistivity versus depth (Figure 5.2) is constructed from the apparent resistivity for each sounding points at different maximum half-current electrode spacing

(AB/2). The selection criteria for this AB/2 values is based on showing the resistivity variation for a number of representative slices. The map shows the distribution of apparent resistivity vertically as well as laterally at different pseudo depths. The apparent resistivity value is seen to generally vary between 2-32 Ω-m. From the sliced stacked map as the pseudo depth increase, the apparent resistivity value is decrease in the western direction. The sliced staked map show that low resistivity, which is less than 14 Ω-m exist in the southwestern corner except at depth of AB/2=100. High resistivity observed on northeast direction and center of the map at the resistivity value is greater than 26Ω-m.

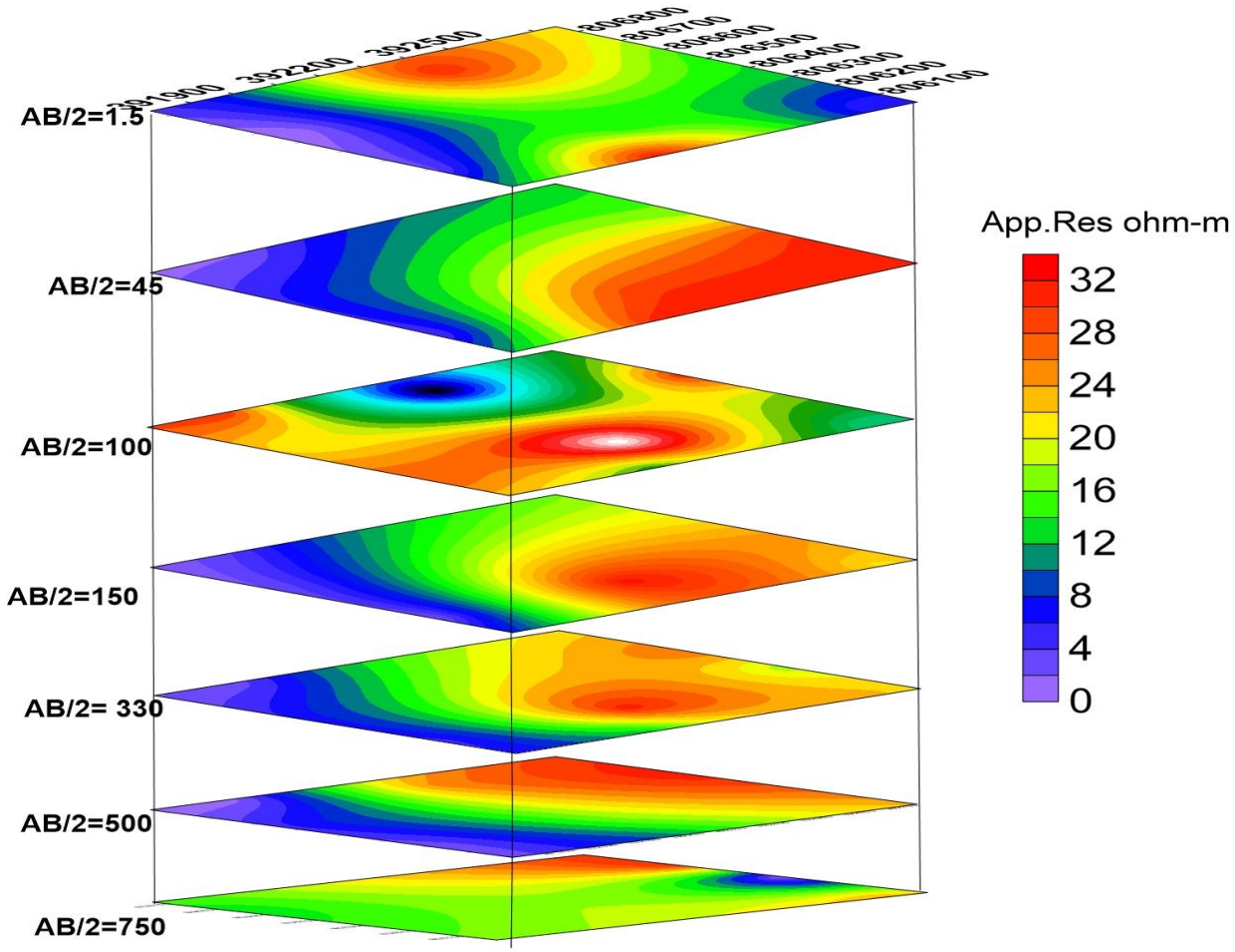

Figure 5.2 Sliced-stacked map of various AB/2

5.1.2 Pseudo depth section along line- 1

The pseudo depth section map is one form of presenting electrical resistivity value of the subsurface material. The map is produced by using surfer 10 software with electrical resistivity

data and showing high or low anomaly value.

The pseudo depth section map is generated from the three VES of VES-1, 2 and 3 that lie along Line-1, is shown the in Figure 5.3. This survey line in the study area, which is passes over the main thermal spring manifestation areas. From the pseudo depth section map, the top part of the section, in relative terms, shows that intermediate resistivity and the middle part of the horizon mapped over all the VES points along the line is low resistivity whereas the bottom horizon is of high resistivity response; especially in the VES-2 relatively high resist materials exist. Overall, the resistivity values generally is range from 1.5 -16.5 Ω-m. A continuous and horizontal low apparent resistivity anomalous zone with resistivity range 1.5-5.5 Ω-m is observed along Line-1 over pseudo depths of 50-550m. The low resistivity value is indicate that the existence of low resist subsurface material.

From the pseudo depth section map, it shows that vertical variation in resistivity and as the depth increase the resistivity also increase, at the depth of 400-750m. The subsurface material in this profile line is highly affected by the geothermal fluid due to resistivity value low is observed. In general, the resistivity value in this profile is low but the resistivity value show considerable variation with depth.

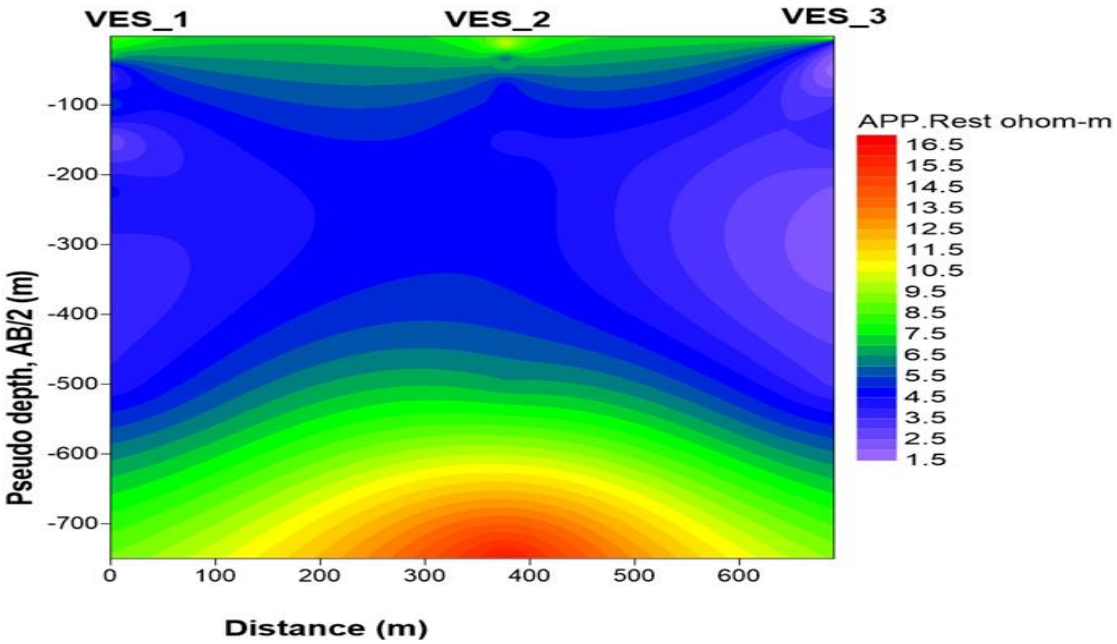

Figure 5.3 Pseudo depth section map of Line -1

5.1.3 Geoelectrical section along Line- 1

The geoelectrical section plot (Figure 5.4) are constructed from interpreted layer parameter of the three VES laying along Line-1 and borehole data. The interpreted layer parameter of the VES are given in Appendix-1 and the borehole depth lithological description presented on Appendix-2.

According to geoelectrical section map along Line-1 have five layer with different resistivity value are observed. The top most part is described as water saturated clay with resistivity of 6.7-12.9 Ω-m. The thickness of this layer is 1.5m in VES-1 and 2 m in VES-2. The layer has low resistivity probably due to the clay is highly saturated with water.

The second horizon on the geoelectric section is represented by fractured/weathered ignimbrite with resistivity of 5.6-11.9 Ω-m. This geological formation has a thickness of 2.1m in VES-2 and 15m in VES-1. The third layer of geoelectrical section represented by tuff formation with resistivity value of 1.4- 13.3 Ω-m .This layer is shown on VES-2 and VES-3 but in VES-1, the layer is not observed. The thickness of the formation is 5m in VES-2 and 25m in VES-3. In this layer weak zone is observed and important for geothermal to conduit water.

The fourth horizon on the geoelectric section represented by resistivity of 2.5 – 6.4 Ω-m and the geological formation is ash. The layer is with a thickness of 65.5m in VES-3 and 140.8m in VES-1. The bottom part of the subsurface is represented by slightly weathered ignimbrite with resistivity of 1-7 Ω-m.

Generally, the resistivity value of the layer in geoelectrical section line-1 is very low because of the hot spring manifestation is along this profile line and water are highly saline. Therefore, the thermal heat of the Earth affects the subsurface material, and their resistivity value is decrease.

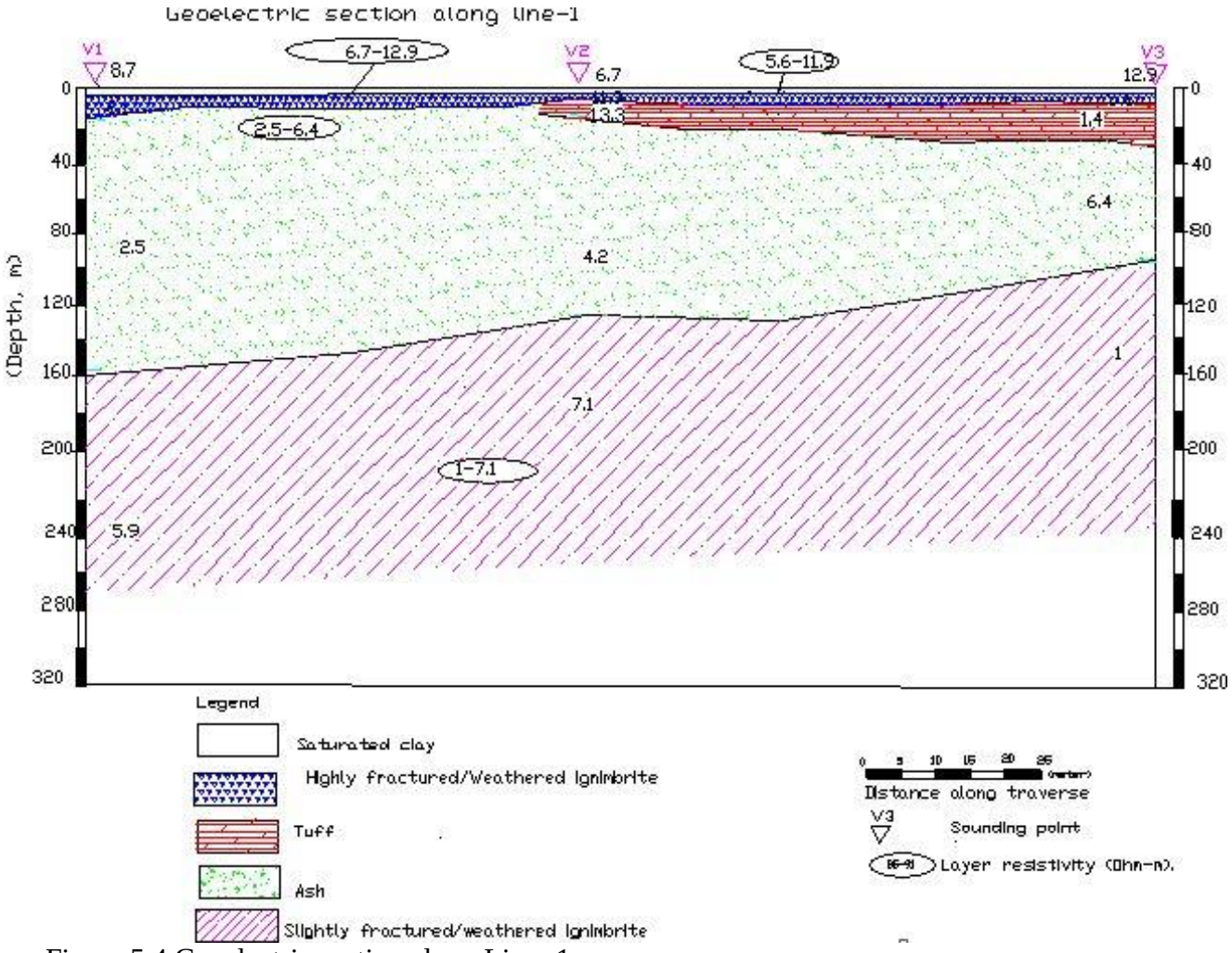

Figure 5.4 Geoelectric section along Line -1

5.1.4 Pseudo depth section along Line-2

The pseudo depth section is constructed from the VES-4, 5 and 6 along Line -2, as shown in the (Figure 5.5). According to the section, high resistivity values are observed at the top of VES-4, VES-5 and bottom part of the VES-6. Low resistivity value observed on the bottom part of VES-4, VES-5 and top and middle part of VES-6. The resistivity value is range from 6- 42 Ω-m. The low and continuous apparent resistivity anomalous zone with resistivity value 6-18 Ω-m observed along Line-2. The map shows a weak zone that oriented approximately in the NE-SW trending on this survey line.

In the pseudo depth map, the apparent resistivity value is decrease with increase in pseudo depth at VES-4 and 5 whereas in the VES-6 the reverse one.

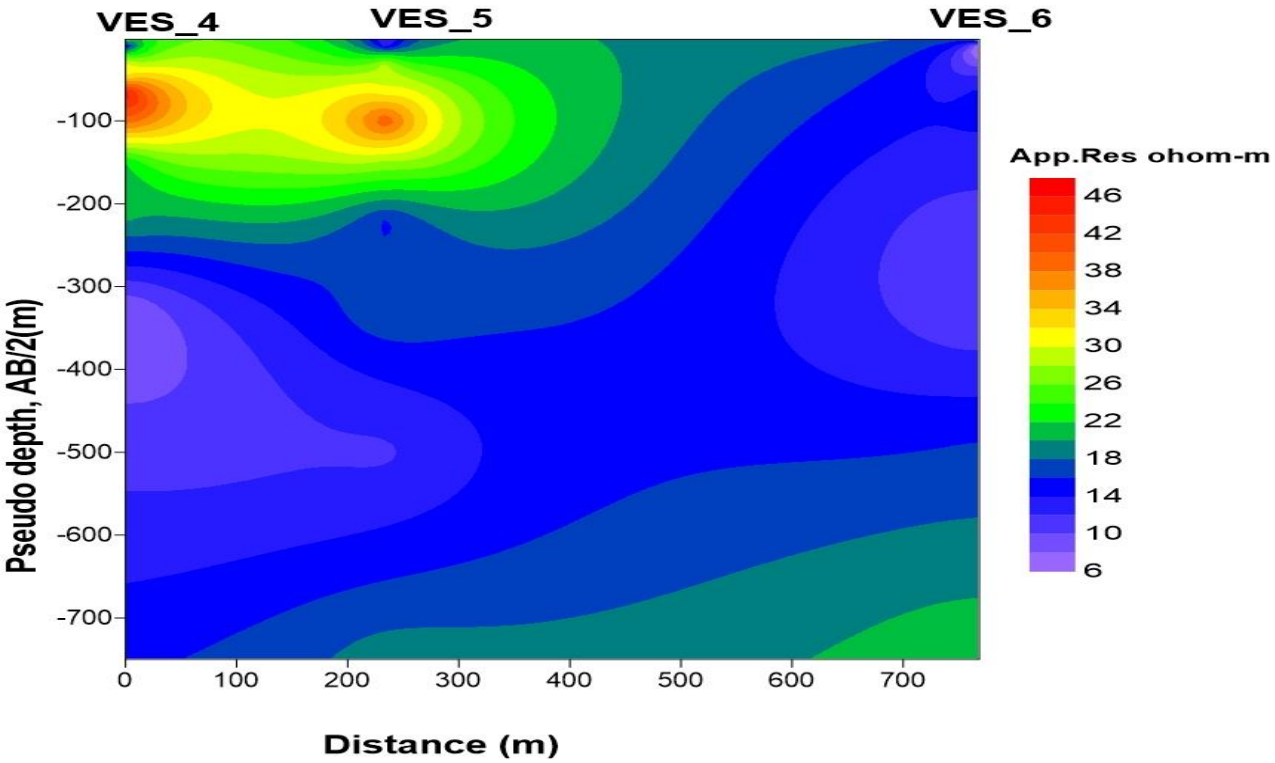

Figure 5.5 Pseudo depth section map of Line-2

5.1.5 Geoelectric section along line-2

The geoelectric section map along Line-2 was compiled from the model parameter VES data points of VES-4, 5 and 6 with the lithological log of the borehole data that are found near the Alaba town. Figure 5.6 shows the geoelectrical section map a long Line-2.

A long Line-2 the subsurface are characterized by five geoelectrical layers. The top two layer have small thickness and not easily visible on the map. The top layer is geologically represented by wet top soil with resistivity varies from 31.9 to 46.3 Ohm-m and at a thickness of the layer 0.5 to 1.1m.

The second layer of the geoelectrical section is represented by resistivity value of 3.7 - 9.7 Ω-m with a thickness of 1.8m around VES-4 and 3.7m around VES-5. This layer is geologically fractured ignimbrite formation and saturated with water due to this the resistivity low as compared to the dry formation. Beneath the second layer, there exist highly resistivity geoelectric layer with a thickness of 22m around VES-4 and 62m around VES-5. This variation

of thickness in the layer indicates that the probability existence of weak zone. The resistivity of this layer ranges from 28.7- 62.3 Ω-m is composed of welded tuff.

The fourth layer of the geoelectric section is represented by 100m a thick horizon around VES-6 and 160m around VES-5, with resistivity value of 5.2-29.3 Ω-m. This layer is geologically represented by ash formation. The fifth layer of the geoelectric section is represented by slightly weathered ignimbrite with resistivity ranges from 10.3-63.1 Ω-m. This layer is the bottom layer and the weak zone is visible on around VES-4.

Generally low resistivity zone is shown on intermediate and second layer of the geoelectric section.

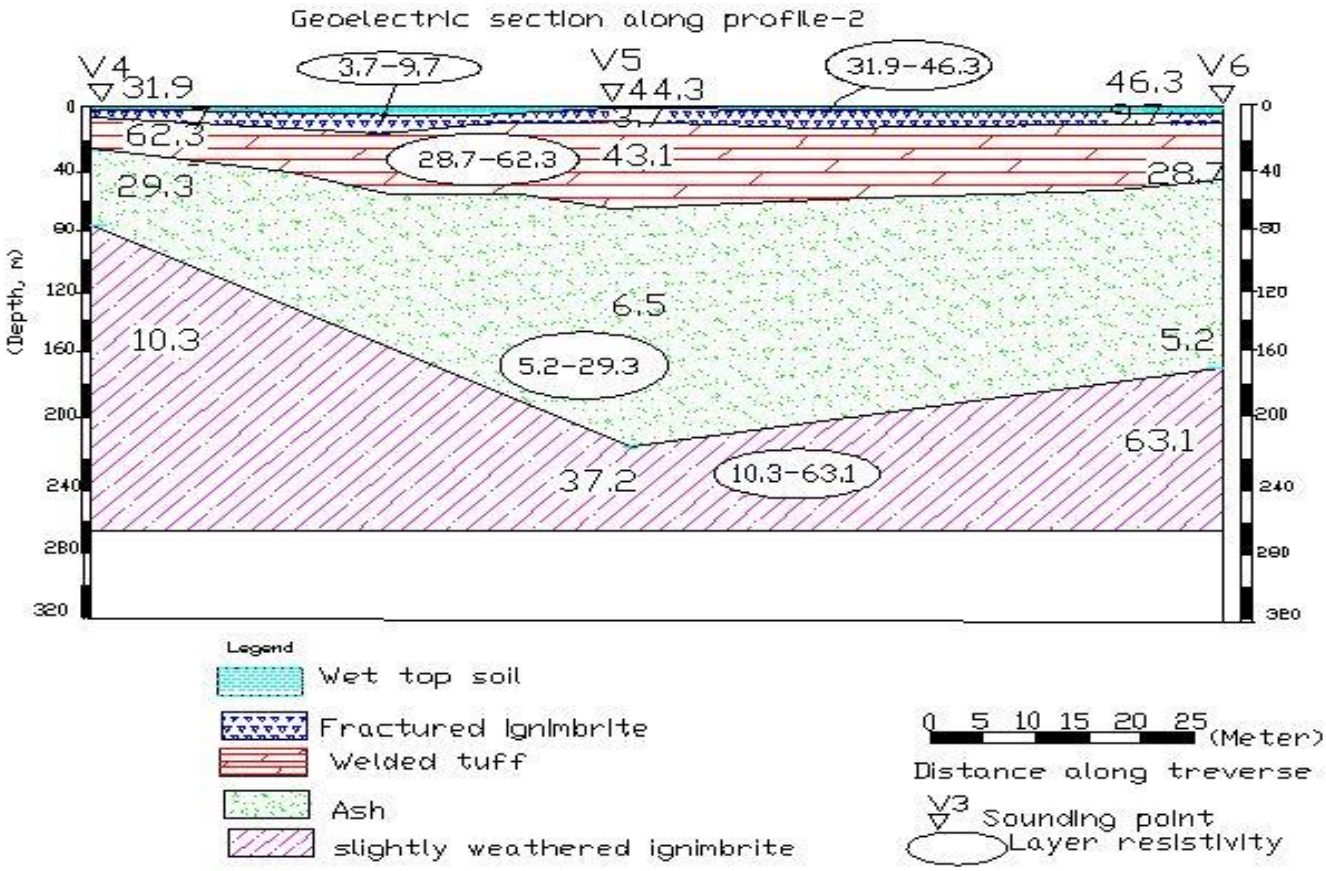

Figure 5.6 Geoelectric section along Line-2

5.1.6 Pseudo depth section along Line-3

The pseudo depth section constructed from VES-7, 8 and 9 that along on survey Line-3 are plotted in Figure 5.7. Low apparent resistivity values are observed on the bottom and middle

horizon of VES-8 and middle part of VES-7 with resistivity value ranges of 6- 15Ω-m. High resistivity value exist in the top part of VES-7, VES-8 and VES-9, bottom part of VES-7 and VES-9 with resistivity value 18-36 Ω-m. In the overall resistivity value ranges from 6- 36 Ω-m.

Generally, the pseudo depth map shows lateral and vertical variation of the subsurface due to the resistivity. The presence of weak zone is important for fluid transportation and circulation.

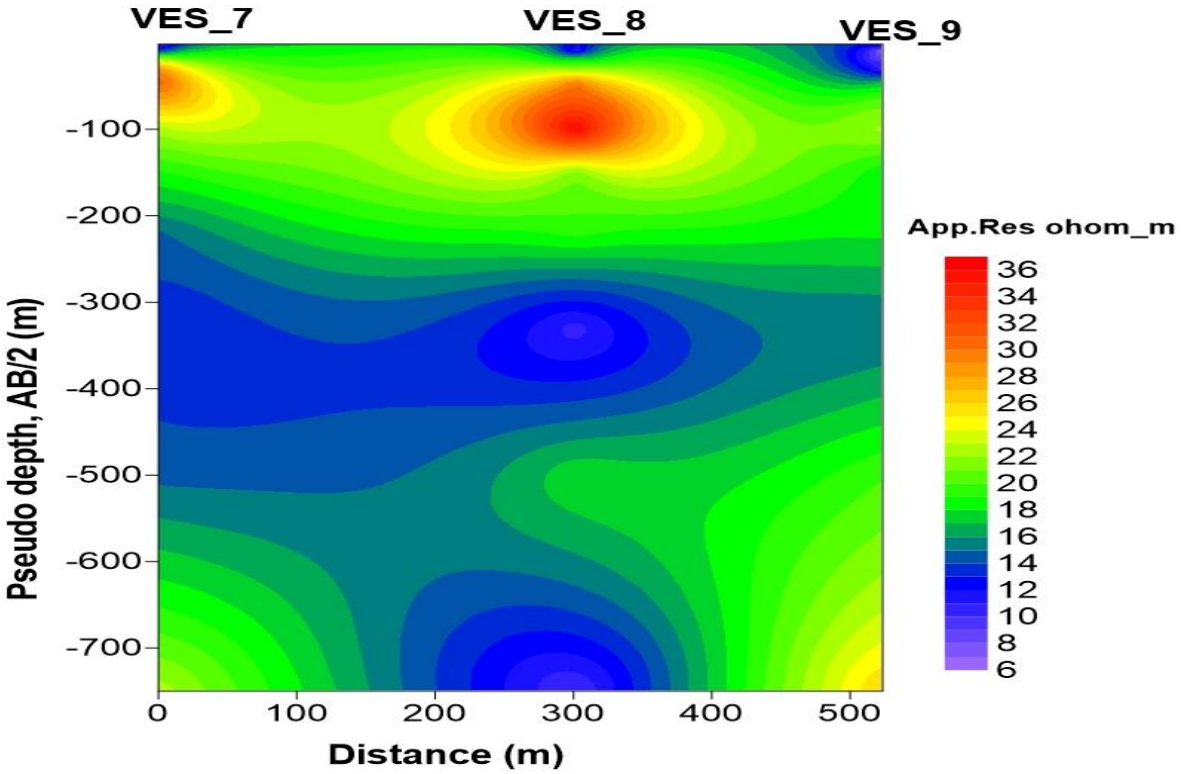

Figure 5.7 Pseudo depth section map a long Line-3

5.1.7 Geoelectric section a long line 3

The geoelectrical section map (Figure 5.8) constructed from the model parameter of VES-7, 8 and 9. This geoelectric section generally consist of five layer with different resistivity values. The top most layer is with resistivity of 10.4-22.1 Ω-m and a thickness of 0.7m around VES-8 and 2.3m around VES-9, the thickness of this layer is almost uniform in all VES data points. The layer is geologically represented by the clay formation. The formation is varies in resistivity due to variation in moisture content in the clay unit.

The second geoelectrical layer is a thickness of 1.5m around VES-7 and 6.7m around VES-9, with resistivity varies 3.6-5.8 Ω-m. The layer is geologically highly weathered ignimbrite formation. The third geoelectric layer is increase in thickness and resistivity as compared to second layer. The thickness of this layer 27.9m around VES-7 and 56.7 m around VES-8, with a resistivity of 39.6 - 51.2 Ω-m. This formation is characterized by tuff.

The fourth geoelectrical layer is a thickness of 152.7m around VES-9 and 259.9m around VES-8 with resistivity of 7.7 - 10.6 Ω-m. This layer geologically is characterized by ash formation. In this layer, resistivity is decrease due to the weathering and fracturing of the rock and weak zone is observed. This weak zone also observed in the pseudo depth section map in bottom part of VES-8 and VES-9. The bottom of the geoelectric layer have a resistivity range from 11- 59.4 Ω-m. This layer may be interpreted as slightly weathered ignimbrite.

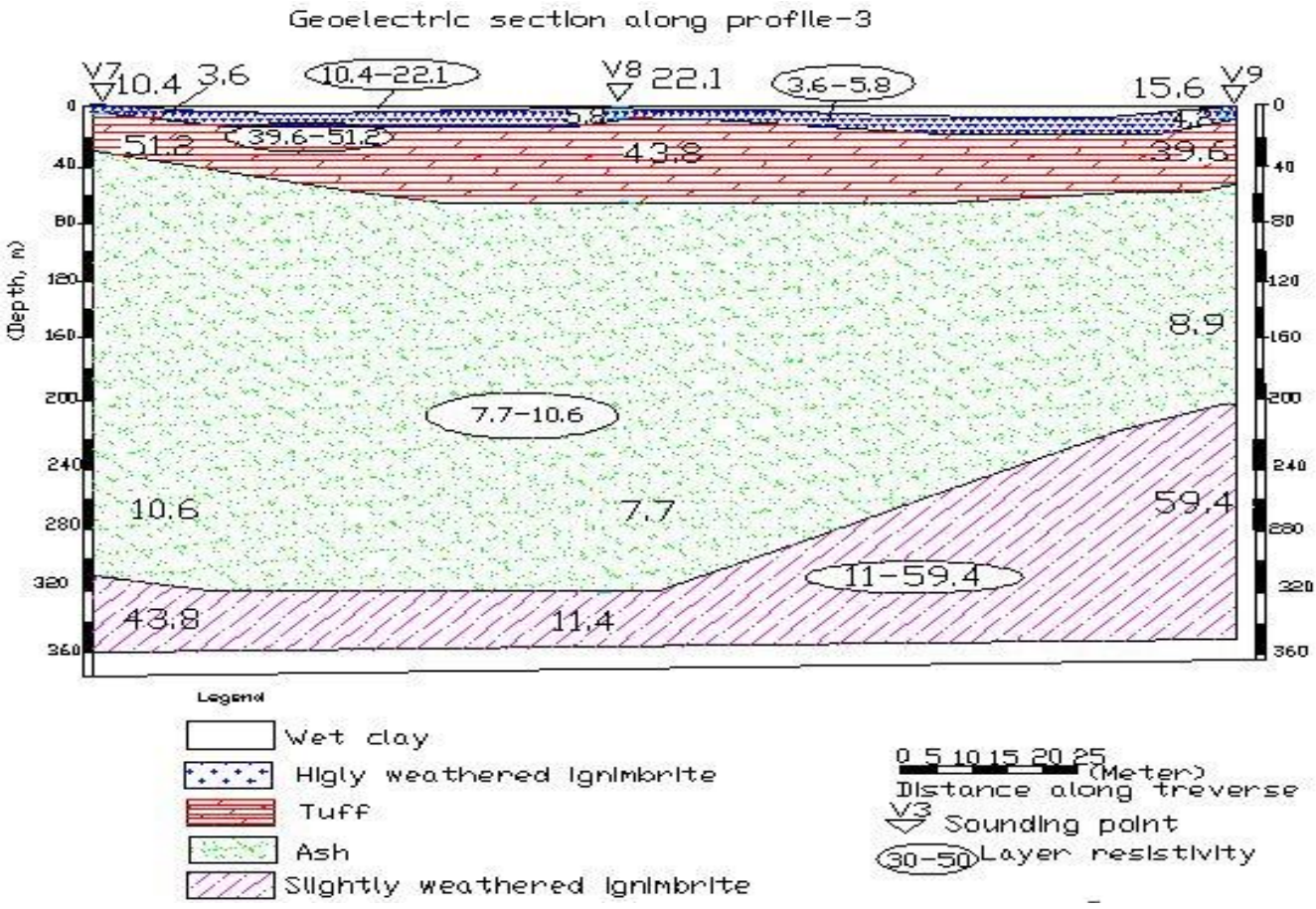

Figure 5.8 Geoelectric section along Line-3

5.1.8 Pseudo depth section along Line-4

Figure 5.9 show the pseudo depth section of a long Line-4 constructed from VES-2, 5 and 8. From the pseudo depth section map, low resistivity value are observed in the top to bottom of VES-2 and bottom part of VES-5 and VES-8 with apparent resistivity of 4-18 Ω-m. High resistivity value observed top part of VES-5 and 8 at the resistivity of 20-32 Ω-m. This map show lateral variation of the subsurface but negligible in vertical variation. The resistivity value range from 4-36 Ω-m.

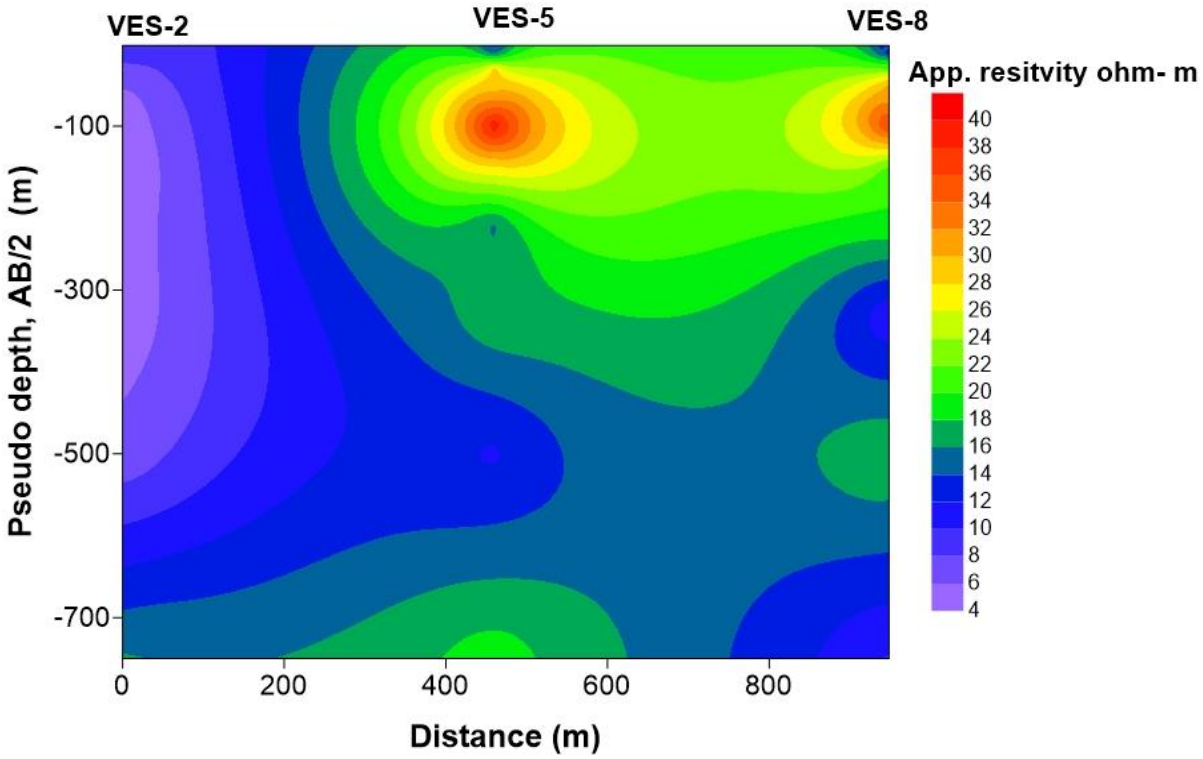

Figure 5.9 Pseudo depth section map of a long Line-4

5.2 Magnetic data result and interpretation

The aim of magnetic survey is to identify the presence of weak zones, structures and variation in lithology in the subsurface that are related with regions of magnetic anomalies. To facilitate this interpretation, the result of magnetic data are presented in the form of different maps that have been generated after the field data has been corrected and processed.

5.2.1 Magnetic anomaly profile

Magnetic anomaly can be interpreted qualitatively and quantitatively. The interpreted anomaly can be presented in the form of map and profile.

Figure 5.10 shows that the residual magnetic anomaly profile along Line-1, which indicate the minimum and maximum anomaly value of -9nT and 14nT at distance of 32m and 30m respectively. The profile shows an abrupt increase anomaly value of 14nT at distance of 30m and it indicates that the weak zone and also depicted in resistivity section.

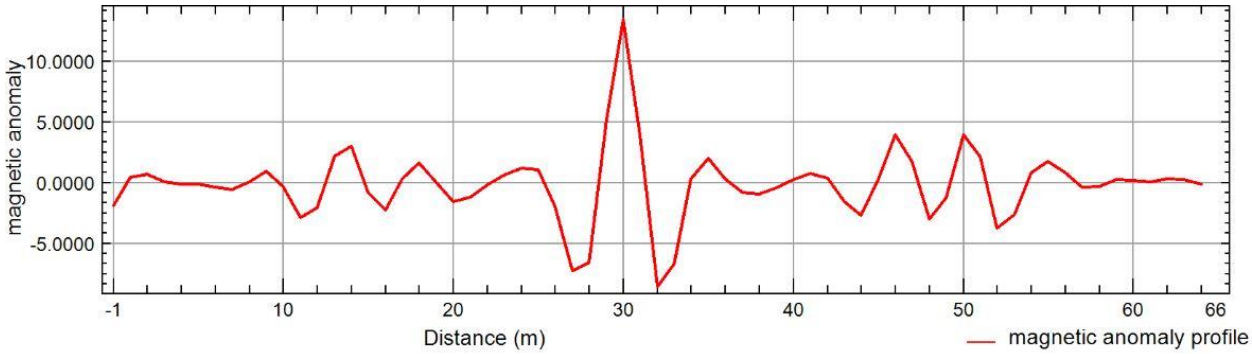

Figure 5.10 Residual magnetic anomaly profile along Line-1

The residual magnetic anomaly profile a long Line-2 is depicted in Figure 5.11. This residual magnetic profile shows small variation of magnetic anomaly but at distance of 35m high magnetic anomaly value of 8nT. At the place of abrupt change of magnetic anomaly, there exist a weak zone.

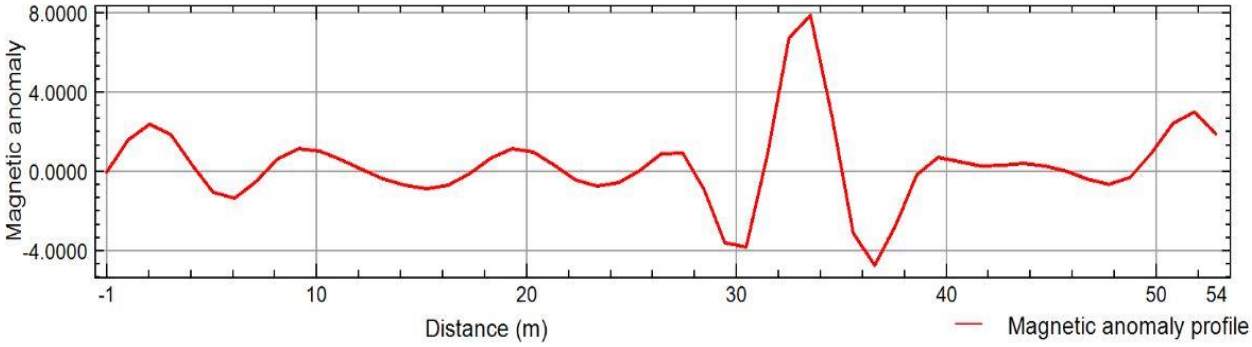

Figure 5.11 Residual magnetic anomaly profile along Line-2

5.2.2 Total magnetic anomaly map

It has been discussed in the previous sections that magnetic data has been obtained over six survey lines that the total magnetic anomaly map (Figure 5.12) is produced from the magnetic field data after making the diurnal and IGRF corrections. The map shows the overall variation of magnetic responses of the subsurface possible structures.

The total magnetic anomaly intensity ranges from -244nT to 68nT. This anomaly varies with positive and negative intensity due to dipolar nature of the causative body. To interpret this total magnetic anomaly is difficult due to dipolar. Low magnetic anomaly observed in the study area with range value (-244 to-167nT) north, North West, west, southeast, northeast direction and central part of the map. High magnetic anomaly exist in the west and east part of the area while intermediate anomaly observed on central part. This high magnetic anomaly is probably due to the presence of highly magnetized material. The hot spring in the study area manifested in the top corner at the center and bottom corner in the left direction.

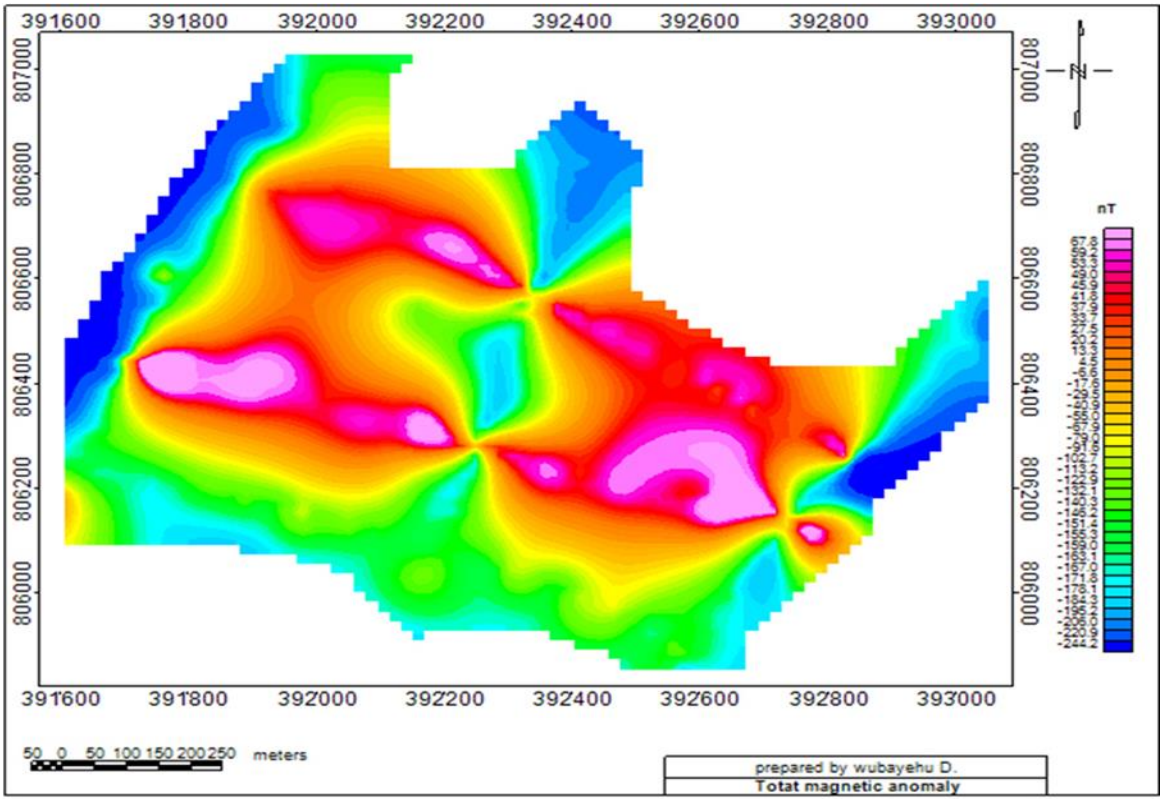

Figure 5.12 Total magnetic anomaly map, Arto thermal springs, Alaba, Main Ethiopian Rift

5.2.3 Residual magnetic field anomaly map

The residual magnetic anomaly map (Figure 5.13) of the study area generated from the total magnetic anomaly map separating from the regional using MAGMAP high pass filter by Geosoft Oasis Montaj (v.7). The prominent geological structure observed in the residual magnetic anomaly map that generally not visible in total magnetic anomaly. The residual magnetic anomaly map shows the effect of shallow mass.

From the map it observed that the residual field intensity value -43 to 46nT, which is large variation this due to lithology, degree of alteration of rock and so on. Low magnetic anomaly ranges -43 to -10nT observed in the northwest direction, southeast and at central part of the map due to the presence of shallow anomaly's body. This low magnetic anomaly coincide with the pseudo-depth section map and geoelectric section map. Therefore, the response of low magnetic anomaly the alteration of hot spring with rock and fracturing of rock.

The Intermediate magnetic anomaly range from (-8 to -0.2nT) in the study area enclose the low magnetic anomaly of northwestern, northern, southern and eastern direction. High magnetic anomaly observed on the NW, southeastern, south and central part of the map. From the residual magnetic map, it shows that the structure trend in the NE-SW and NW-SE direction. This structural feature represent fracture or fault in the study area. More aligned short wavelength magnetic anomaly observed in the residual than the total magnetic anomaly.

In the residual magnetic anomaly map, high local magnetic separated from low magnetic anomaly by linear structural features, which dominantly oriented in NE-SW direction. Figure 5.13 revealed that low anomaly zone covered the four of hot spring manifestation in the area.

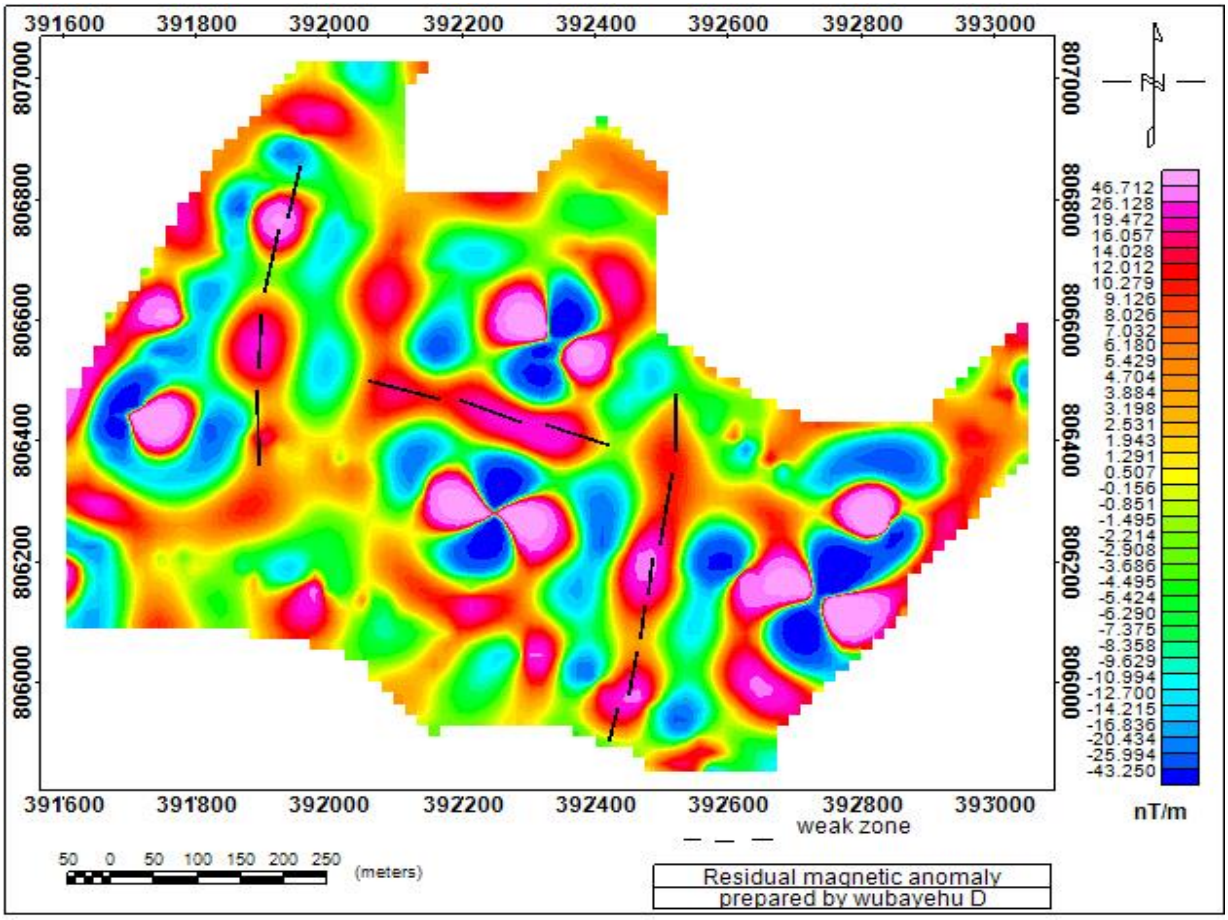

Figure 5.13 Residual magnetic anomaly map, Arto thermal springs, Alaba, Main Ethiopian Rift.,

5.2.4 Analytical signal map

Analytic Signal or total gradient is formed through the combination of the horizontal and vertical gradients of the magnetic anomaly and it is applied either in space or frequency domain, generating a maximum directly over discrete bodies as well as their edges. The generated maximum directly over the causative body and depth estimation abilities of this filter make it a highly useful technique for magnetic data interpretation. The maximum can be used to detect the structures responsible for the observed magnetic anomalies over an area (Roest et.al., 1992).

The analytical signal map generated from the residual magnetic anomaly map using MAGMAP Geosoft Oasis Montaj v.7. This map used to identify the horizontal contact and depth of the contact. The analytical signal map over the causative body and contact is high as shown (Figure 5.14). As seen from the map, form of ridge with magnetic anomaly peak are observed on NW,

SE and central part of the map. The peak analytical signal map coincide with high residual magnetic anomaly map. The analytical signal map in the study area follow N-S, NW-SE and NE-SW trend but most of the structure follow N-S trend.

The filter technique for the analytical signal map has a potential to reduce the ambiguity that could arise from the effect of dipolar source. In the study area, which is the hot spring manifested area the analytical signal magnetic map is high magnetic anomaly.

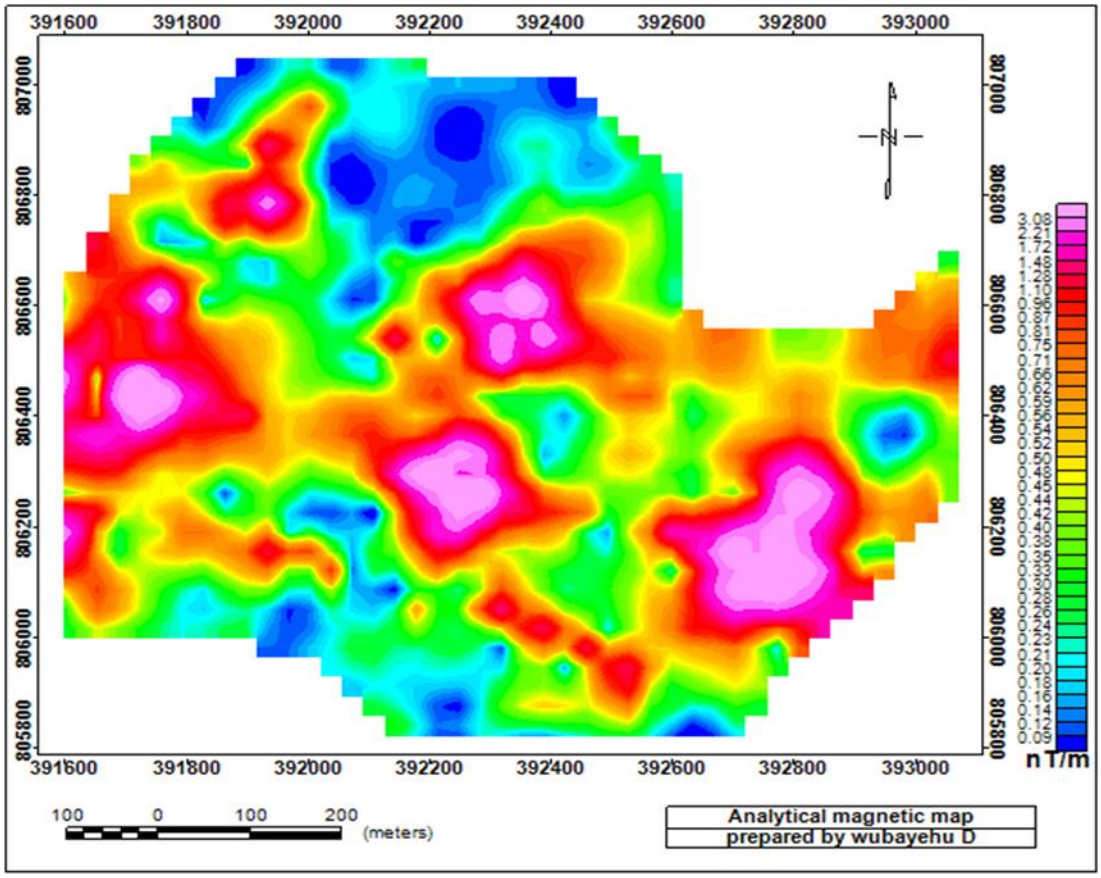

Figure 5.14 Analytical magnetic map, Arto thermal springs, Alaba, Main Ethiopian Rift

5.2.5 Tilt derivative magnetic map

The tilt derivative magnetic map (figure 5.15) of the study area is compiled by applying tilt derivative filter to the analytical signal magnetic anomaly map using Geosoft Oasis montaj v.7 software. This map is supposed easy to identify fault, contact and locate edge geological structure in the study area.

The tilt derivative magnetic map show more detail structural contact/boundary than the residual and analytical signal magnetic anomaly map. Tilt derivative map show the positive over the source, cross through at zero or near on contact or fault and negative outside the source. The study area show structural contact/boundary in NW-SE, NE-SW and N-S trend direction.

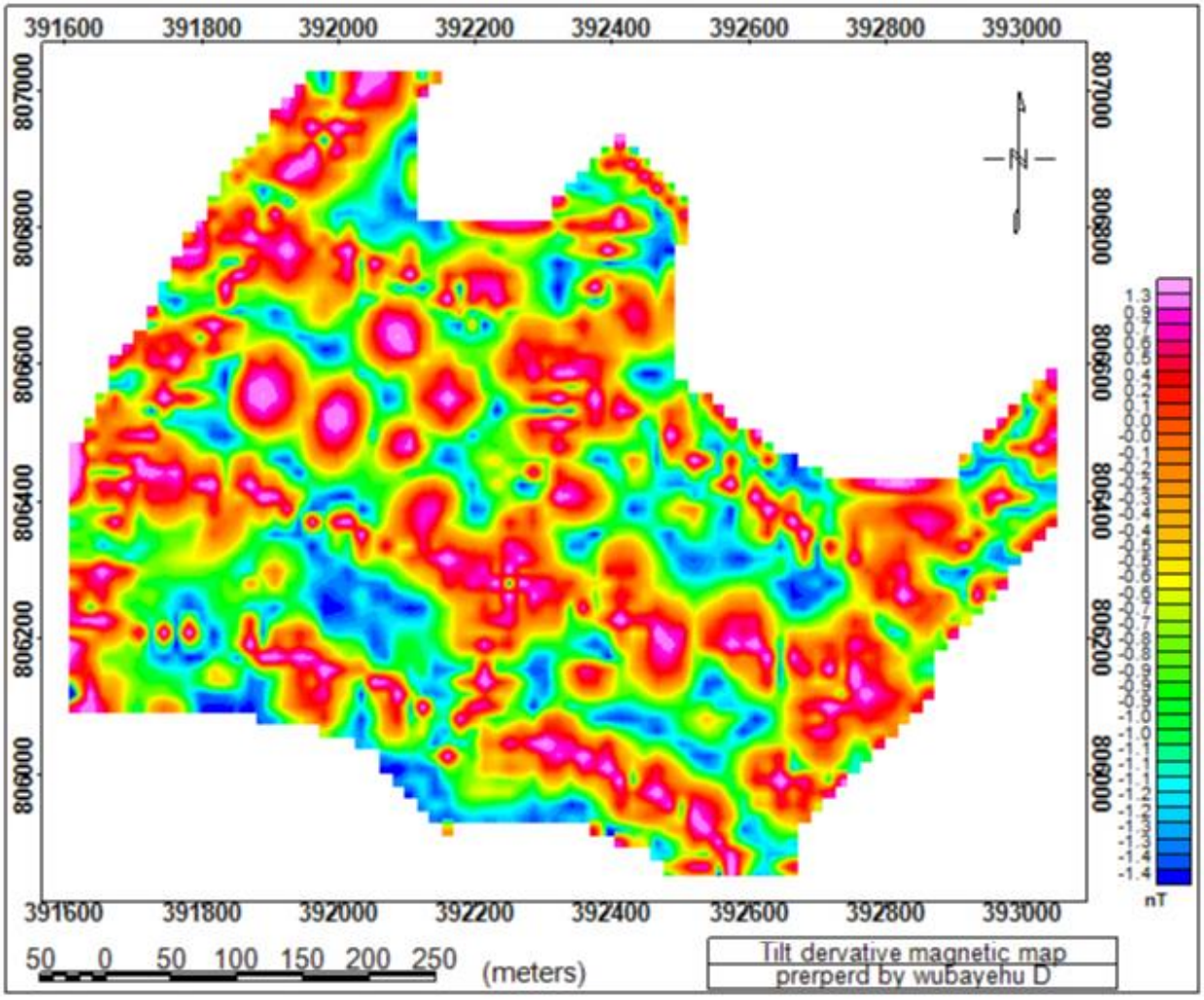

Figure 5.15 Tilt derivative magnetic anomaly map, Arto thermal springs, Alaba, Main Ethiopian Rift.

5.2.6 Euler Deconvolution magnetic map

Euler deconvolution was applied to the residual magnetic anomaly in order to estimate depth and location of magnetic anomaly source. Euler deconvolution map is compiled by standard 3D Euler in the Oasis Montaj software. The Euler deconvolution map prepared by different structural indices (SI= 0, 0.5 1, 2 and 3) and best structural indices is selected by visual

observation of the map compiled from different structural indices. Each structural indices represent different geological feature of contact, fault, dike, sill and sphere.

The depth and location of the anomalous source was estimated by the 3D Euler deconvolution method. This was done first by computing derivative the residual magnetic data then process in the (x, y and z) to get the depth and position of anomaly source. After that, specify the structural Indies.

The Euler deconvolution magnetic map with structural indices SI=2 is as show Figure 5.16 with highly clustering. The light green circle represent source with range greater than 200m depth, which are located in the map southern and southeaster direction. The purple circle represent with the source range 170m-200m depth. At this depth in the map found on north direction. The blue circle represent with source range from 120m-170m depth which shown on map dominantly in northeast and western direction. Green circle represent the source range from 80m-120m depth which shown on the map southeastern and eastern direction. Red circle represent the source range less than 40m depth, which dominantly found on the map in the north direction. From the Figure 5.16, more cluster shown at the depth of less than 40m and 80-120m depth.

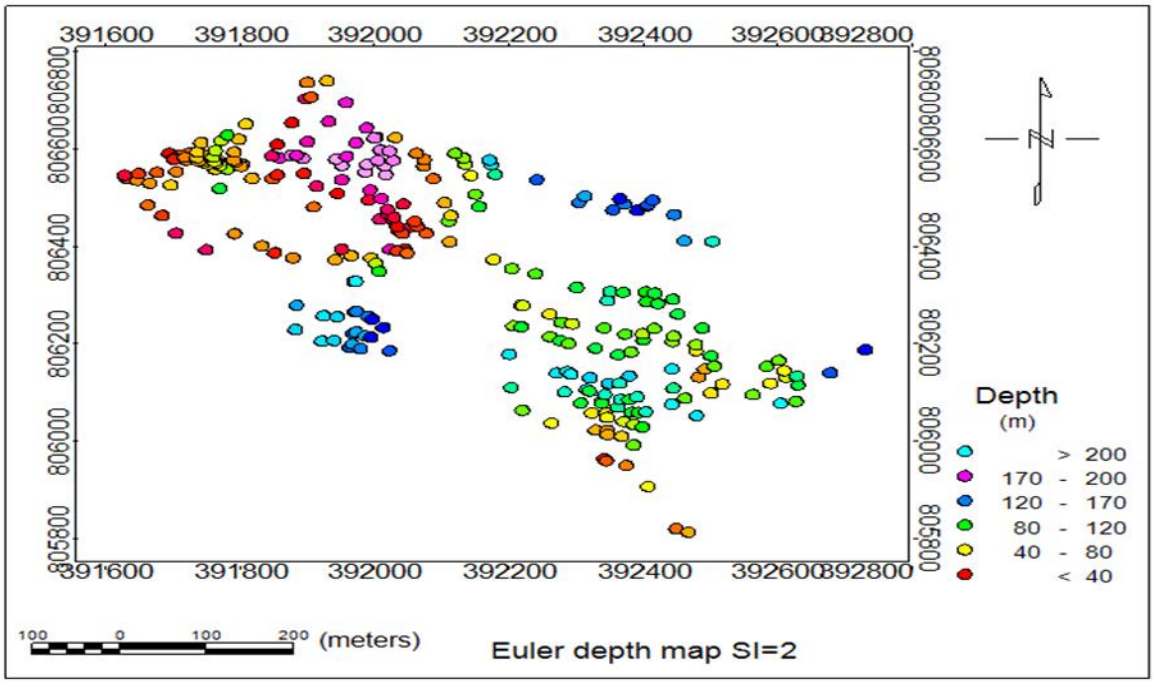

Figure 5.16 Euler deconvolution magnetic map at SI=2

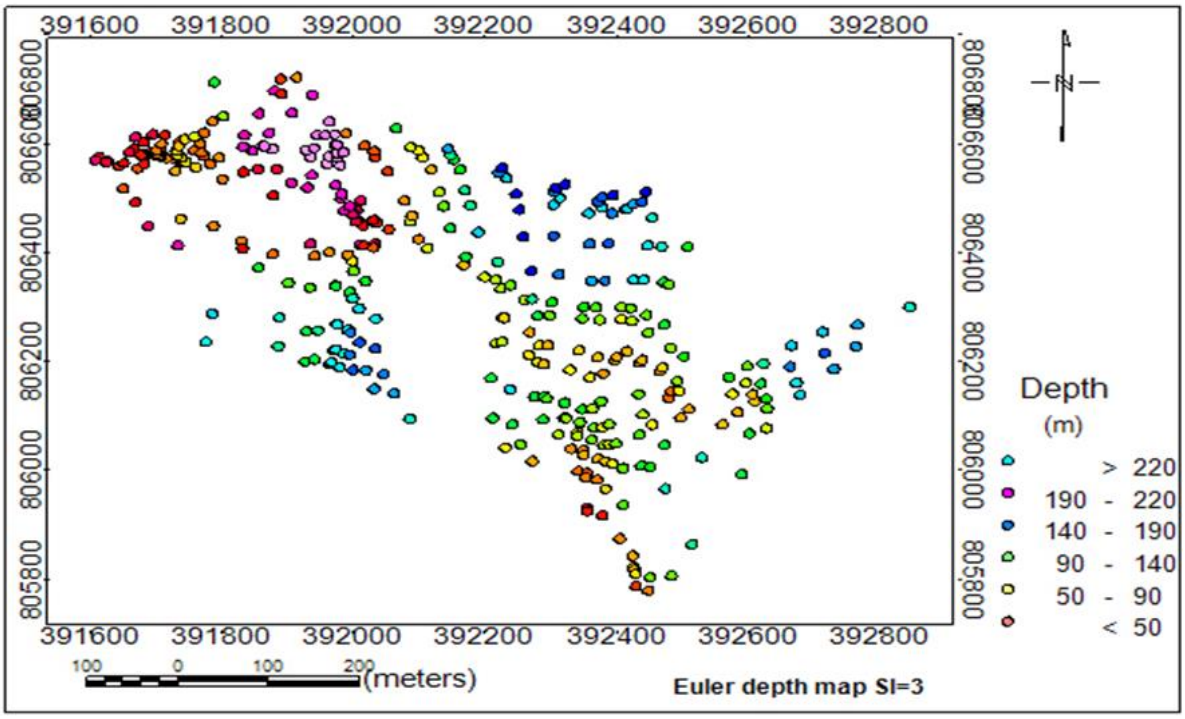

Figure 5.17 Euler deconvolution magnetic map at SI=3

CHAPTER SIX

6 CONCLUSION AND RECOMMENDATION

6.1 Conclusions

This research work is presented the result of integrated geophysical methods in the Arto hot spring, Alaba Woreda, Southern Ethiopia, to characterize the thermal setting and the possible weak zone to conduit the discharge of thermal fluid. Nine vertical electrical sounding and 311magnetic data points were collected in the study area. The resistivity data was presented interims of pseudo depth section map, interpreted VES layer, stacked section map and geoelectrical section map. Magnetic data also presented in the form of total magnetic anomaly, residual magnetic anomaly, analytical signal, tilt derivative and Euler deconvolution magnetic maps. The result of the interpretation summarized below;

From the electrical resistivity survey, low electrical resistivity less than 10Ω m observed on the pseudo depth and geoelectric section map along Line-1 was presented. This result indicate that the rocks are highly fractured, weathered, altered with hot water and the water is saline and mineralized. This survey line was over the main thermal manifestation area because of this reason low resistivity value were observed. In the Line-2, the weak zone is visible on the pseudo depth map as well as the magnetic profile anomaly map. This weak zone may be important for the discharge of hot spring and the recharge area for fluid to the subsurface.

The magnetic map interpretation result shows that the subsurface structure in the study area closely associated with the general trend of Main Ethiopian Rift structure. In general, the structure follows dominantly NE-SW and NW –SE direction.

Lowering of electrical resistivity and magnetic susceptibility is essential to fed up the source of hot spring by the fluid and to discharge the hot spring through the subsurface structure. The Arto hot spring is may be fed up from the deep groundwater and local stream throw the subsurface structures.

The source of the hot spring may be regional deep-seated magmatic intrusion. The result of electrical resistivity and magnetic shows that shallow NE-SW structural trend, which is coincide

with general trend of Main Ethiopian Rift. The existence of shallow anomaly may be because of deep-seated magmatic intrusion with shallow geological structure.

6.2 Recommendation

Based on the result obtained and limitation the following points are recommended;

1) Detailed magnetotelleric (MT) with transit electromagnetic methods (TEM) should be conducted for geothermal exploration due to large depth of penetration than galvanic counterpart (DC resistivity). This will be helpful to produce detail inversion model using electrical resistivity. From this to know the source, reservoir and the cap rock for the thermal spring.
2) The qualitative description of electrical resistivity and magnetic data presented above are limited in the area coverage around the geothermal manifestation, regional gravity and magnetic data will recommended, to knowing the general trend of structure in the subsurface.
3) Detailed geological and local stratigraphy map should be prepared to characterize the geothermal setting.
4) Integrated geophysical investigation with geochemistry and hydrogeology have been recommended to model the heat source.

References

Abera Alemu (1992). The Gravity Field and Crustal Structure of the Main Ethiopian Rift. Report No. **26**. TRITA GEOD 1026. Stockholm, Sweden. P.135

Ayalkibet Mekonnen (2014). Assessment of water harvesting technology effect on downstream water availability using, (case of Alaba special Woreda, Ethiopia). Unpublished MSc thesis, Arba Minch Universtiy, Ethiopia. P.149

Basalfew Zenebe, Mathios Agonafir, Meskerem Teshome, Mekdes Taye, Mekonen Bekele, Mohamed Edris, Getachew Burusa and Ezra Yehualashet (2012). Geology, geochemistry and gravity survey of the Hosaena area. Unpublished technical report. P. 68

Berhanu Gizaw (2008). Geothermal exploration and development in Ethiopia. Geothermal training programme, 30th Anniversary Workshop, United Nation University. P. 12

Bitsiet Dereje and Dessie Nedaw (2019). Groundwater Recharge Estimation Using Wet Spass Modeling in Upper Bilate Catchment, Southern Ethiopia. Momona Ethiopian Journal of Science (MEJS). **11**(1):37-51.

Boccaletti, M., Bonini, M., Mazzuoli, R., Bekele Abebe, Piccardi, L., Tortorici, L. (1998). Quaternary oblique extensional tectonics in the Ethiopian Rift (Horn of Africa). *Tectonophysics*, **287**: 97–116.

Bonini, M., Corti, G., Innocenti, F., Manetti, P., Mazzarini, F., Tsegaye Abebe and Pecskay, Z. (2005). Evolution of the Main Ethiopian Rift in the frame of Afar and Kenya rifts propagation. Tectonics. **24**(1)

Brhanu Gizaw (1985). The chemistry of geothermal fluids in geothermal areas of the Lakes District, Ethiopian Rift Valley. UNU geothermal training program Iceland.

Corti G., Manetti P., Tsegaye Abebe, Bonini M. and Mazzarini F. (2008). The volcano-tectonic activity of the Main Ethiopian Rift (East Africa): insights into the evolution of continental rifting. *Actavulcanologica. **20**: 1-2*

Corti, G. (2009). Continental rift evolution: from rift initiation to incipient break-up in the Main Ethiopian Rift, East Africa. *Earth- Science Reviews* **96**(1):1-53.

Ebinger C and Casey M., (2001) Continental breakup in magmatic provinces: an Ethiopian example, *Geology* **29**. 527-530.

Ethiopian Institute of Geological Survey (EIGS) (2012). Geology geochemistry and gravity survey of the Hosaina area. Unpublished technical report. Memoir **no** 36.

Fitch A.A (1981). Development in geophysical exploration method-2, London. P 241.

Giday Woldegabriel, Aronson, J. L. and Walter, R. C. (1990). Geology, geochronology, and rift basin development in the central sector of the main Ethiopia rift. Geological Society of America Bulletin, **102**(4): 439-458.

Kana J.D., Djongyang N., Raidandi D., Nouck P.N. and Dadje A. (2015). A review of geophysical methods for geothermal exploration. *Renewable and Sustainable Energy Reviews*. **44**:87-95

Kazmin, V., Seife Michael Berhe, Nicoletti, M. and Petrucciani, C. (1980). Evolution of the northern part of the Ethiopian Rift. Accad. Naz. Lincei, Rome, **47**: 275–291.

Kearey, P., Brooks, M. and Hill, I. (2002). An Introduction to Geophysical Exploration, third edition. *Blackwell Science Ltd* .p 281

Mahatsente, R., Jentzsch, G., Jahr, T. (1999). Crustal structure of the Main Ethiopian Rift from gravity data: 3-dimensional modeling. *Tectonophysics*, **313**, 363–382

Manzella, A. (2000). Geochemical and geophysical methodology in geothermal exploration geophysical method in geothermal exploration. *Conference proceeding*. Pp 48

Boccaletti M., Bonini M., Mazzuoli R, Bekele Abebe, Piccardi L. and Tortorici L. (1998). Quatemary oblique extensional tectonics in the Ethiopian Rift (Horn of Africa). Tectonophysics **287**: 97-116

Mary, H.D and Mario, F, (2004). What is geothermal energy? : Pisa, Italy, Istituo di Geoscience e Georisorse, p. 65

Meseret Teklemariam, Battaglia, S., Gianelli, G. and Ruggieri, G. (1996). Hydrothermal alteration in the Aluto-Langano geothermal field, Ethiopia. *Geothermics*, **25**(6): 79-702.

Meseret Teklemariam, Kibret Beyene, Yiheyis Amde Berhan and Zewde Gebregziabher (2000). Geothermal development in Ethiopian. *Proceedings World Geothermal Congress*. P 475-480.

Meseret Teklemariam and Kibret Beyene (2005). Geothermal Exploration and Development in Ethiopia. *In: Proceedings World Geothermal Congress*, Antalya, Turkey.

Meseret Teklemariam (2006). Overview of geothermal resource utilization and potential in East Africa Rift System. Short course on surface exploration for geothermal studies. P. 60

Minissale,A. ,Corti,G., Tassi, F. , Darrah, T.H., Vaselli, O., Montanari, D., Montegrossi,G., Gezhagn Yirgu, Selmo, E. and Asfaw Teclu (2017). Geothermal potential and origin of natural thermal fluids in the northern Lake Abaya area, Main Ethiopian Rift, East Africa, *Volcanology and Geothermal Research* **336**:1-18

Mohr, P. (1962). The Ethiopian Rift System. Bulletin of the Geophysical Observatory of Addis Ababa. **5**: 33–62.

Mohr, P.A., (1967). The Ethiopian rift system. Bulletin of the Geophysical Observatory Addis Ababa **11**, 1–65.

Reynolds, J.M., (2011). An introduction to applied and environmental geophysics, 2nded. Wiley-Blackwell. P.778

Tadiwos Chernet (2011). Geology and hydrothermal resources in the northern Lake Abaya area (Ethiopia). J. *Afr. Earth Sci*. **61**, 129–141

Tamiru Alemayehu (2006). Ground water occurrence in Ethiopia. Addis Ababa University, Ethiopia. P.107

Tamiru A. Abiye and Tigistu Haile (2008). Geophysical exploration of the Boku geothermal area, Central Ethiopian Rift. *Geothermics* **37**: 586–596

Telford, W.M., Geldart, L.P. and Sheriff, R. E. (1990). Applied geophysics second edition. Cambridge university press, New York port Chester Melbourne Sydney. P 744

Tesfaye Tessema (2015). Groundwater potential evaluation based on integrated GIS and remote sensing techniques, in Bilate river catchment: south rift valley of Ethiopia. *American Scientific Research Journal for Engineering, Technology, and Sciences*. **10**: 85-120

Selamawit Worku (2016).Sub-surface geology, hydrothermal alteration and 3D modelling of wells LA-9D and LA-10D in the Aluto -Langano geothermal field, Ethiopia. Published MSc Thesis, United Nations University, *Geothermal Training Programme*. p.83

Sintayehu Legesse (2009).integrated hydrogeological investigation of upper Bilate river catchment: southwestern escarpment of Main Ethiopian Rift. Unpublished Msc thesis, Addis Ababa University. P.126

United Nations Development Program (UNDP) (1973): Investigation of geothermal resources of Power development Geology, Geochemistry and Hydrology of hot springs of the East African Rift System within Ethiopia. DP/SF/UN 116-technical report, United Nations, New York, 275

Yahya Ali and Tigistu Haile (2017). 2D resistivity imaging and magnetic survey for characterization of thermal springs: A case study of Gergedi thermal springs in the northwest of Wonji, Main Ethiopian Rift. *Journal of African Earth Science*. **133**: 95-103

José Rivas (2009). Gravity and magnetic methods. Presented at Short Course on Surface Exploration for Geothermal Resources, organized by UNU-GTP and LaGeo, in Ahuachapan and Santa Tecla, El Salvador.

Appendix

Appendix 1: interpreted VES curves for each sounding points

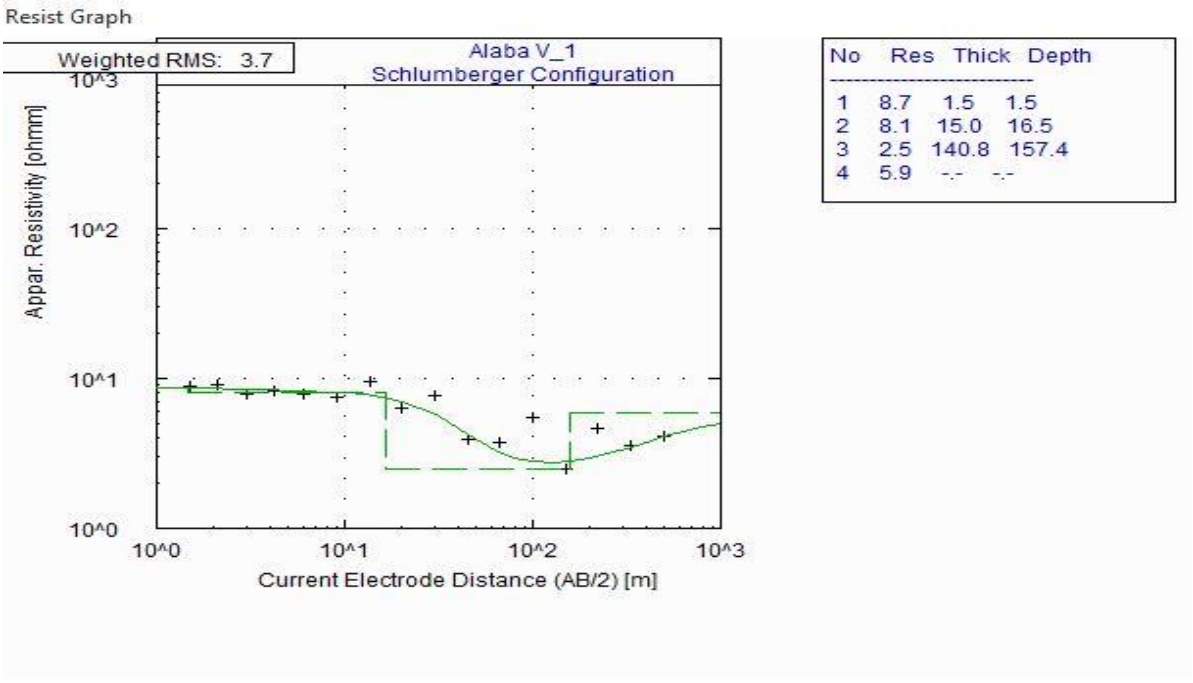

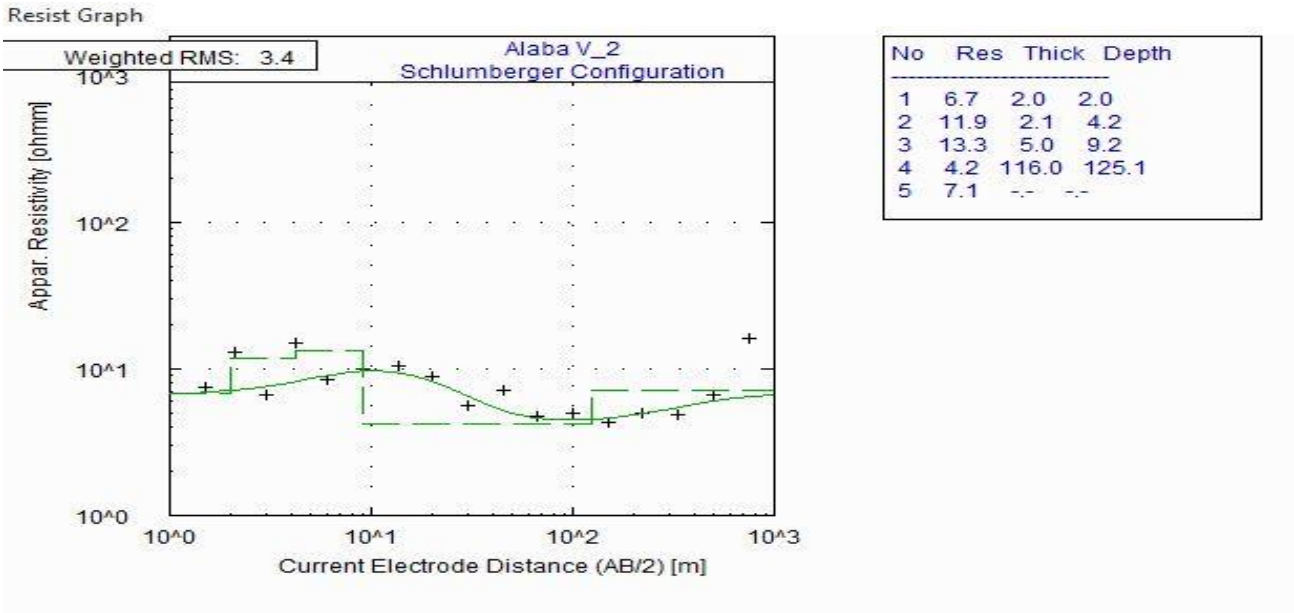

Resist Graph

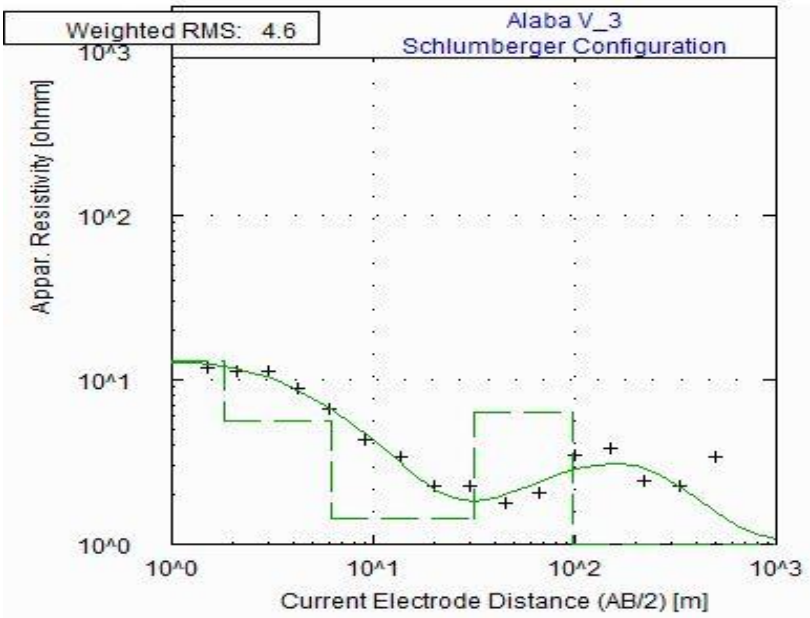

No	Res	Thick	Depth
1	12.9	1.8	1.8
2	5.6	4.4	6.2
3	1.4	25.8	31.9
4	6.4	65.4	97.3
5	1.0	-.-	-.-

Resist Graph

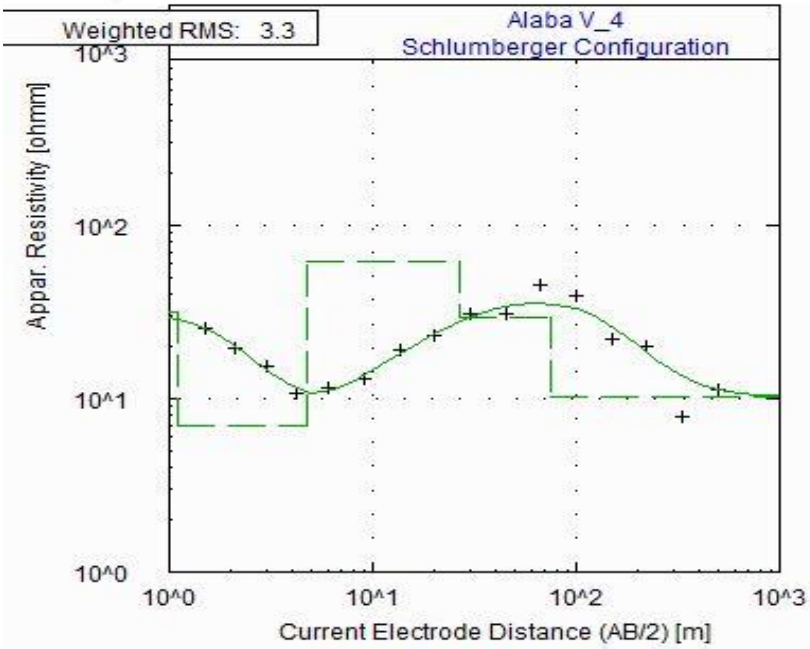

No	Res	Thick	Depth
1	31.9	1.1	1.1
2	7.0	3.7	4.8
3	62.3	22.0	26.8
4	29.3	47.9	74.6
5	10.3	-.-	-.-

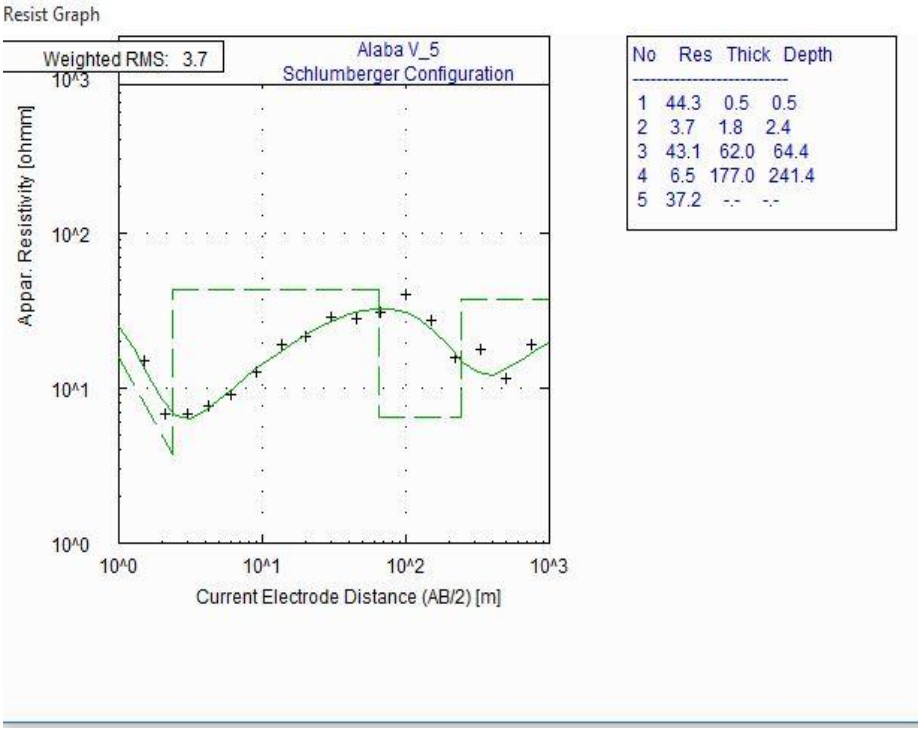
Resist Graph
Weighted RMS: 3.7
Alaba V_5
Schlumberger Configuration
Appar. Resistivity [ohmm]
10^3
10^2
10^1
10^0
10^0
10^1
10^2
10^3
Current Electrode Distance (AB/2) [m]
No Res Thick Depth
1 44.3 0.5 0.5
2 3.7 1.8 2.4
3 43.1 62.0 64.4
4 6.5 177.0 241.4
5 37.2 -.- -.-

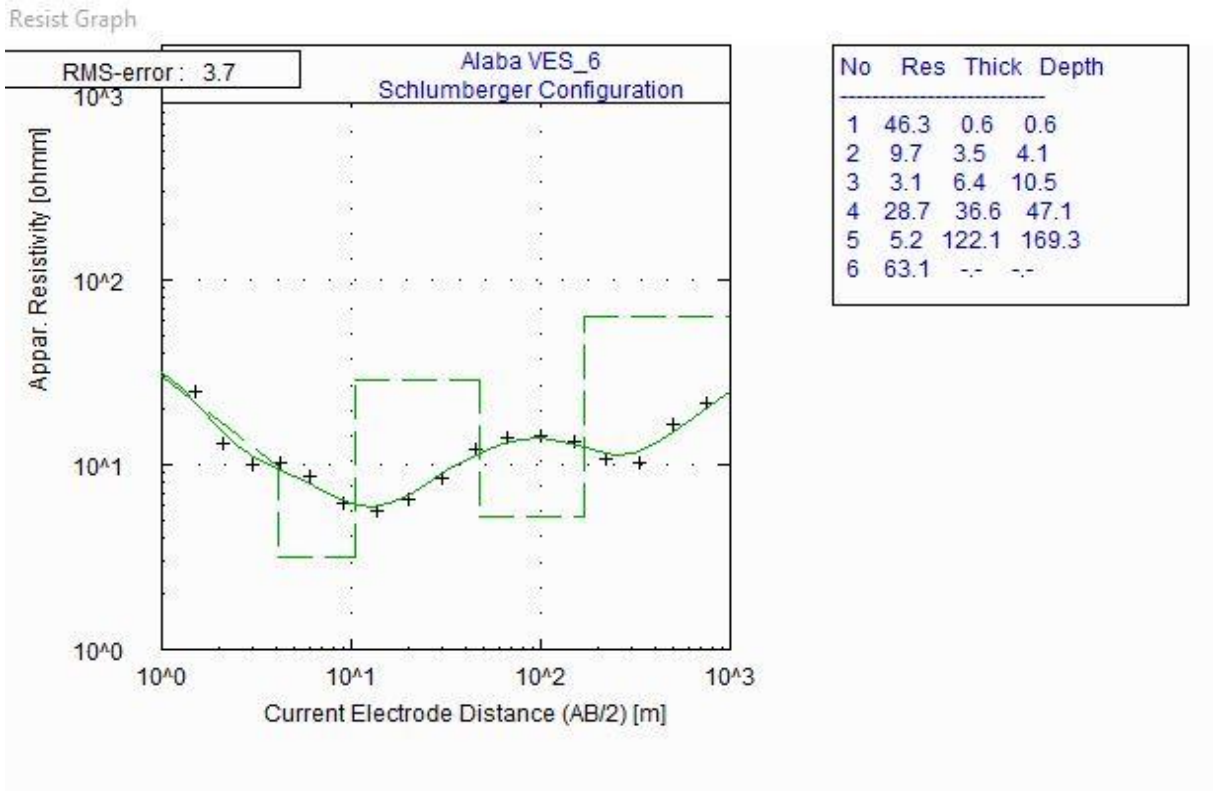
Resist Graph
RMS-error : 3.7
Alaba VES_6
Schlumberger Configuration
Appar. Resistivity [ohmm]
10^3
10^2
10^1
10^0
10^0
10^1
10^2
10^3
Current Electrode Distance (AB/2) [m]
No Res Thick Depth
1 46.3 0.6 0.6
2 9.7 3.5 4.1
3 3.1 6.4 10.5
4 28.7 36.6 47.1
5 5.2 122.1 169.3
6 63.1 -.- -.-

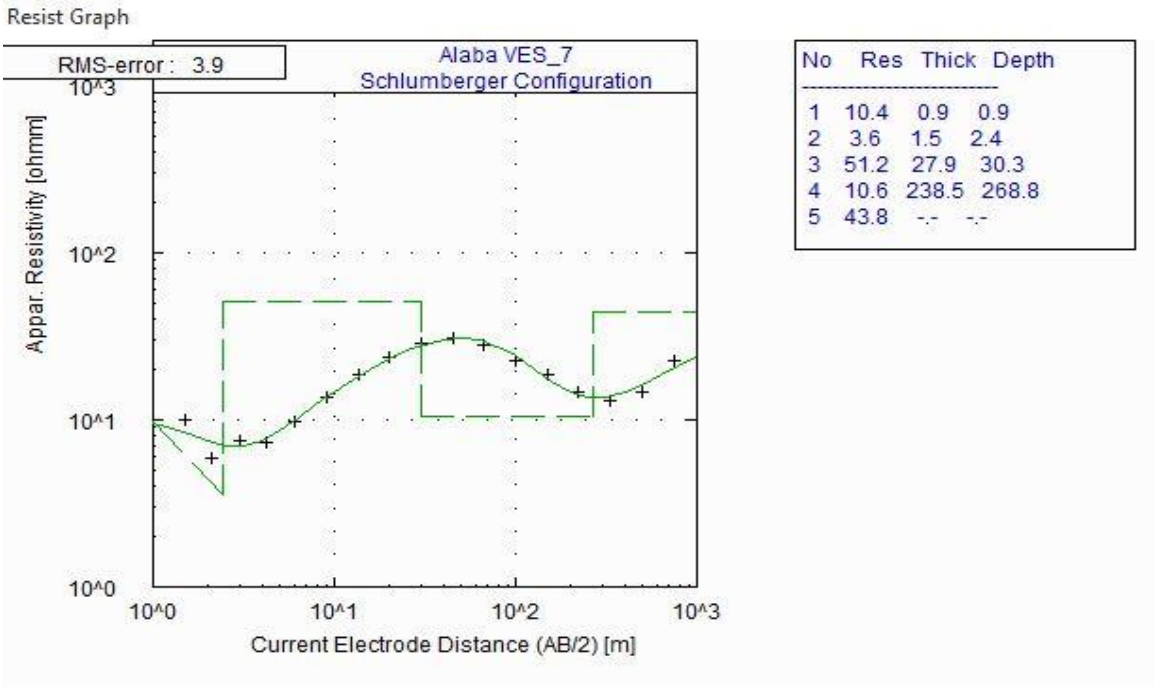
Resist Graph
RMS-error : 3.9
Alaba VES_7
Schlumberger Configuration
Appar. Resistivity [ohmm]
10^3
10^2
10^1
10^0
10^0
10^1
10^2
10^3
Current Electrode Distance (AB/2) [m]
No Res Thick Depth
1 10.4 0.9 0.9
2 3.6 1.5 2.4
3 51.2 27.9 30.3
4 10.6 238.5 268.8
5 43.8 -.- -.-

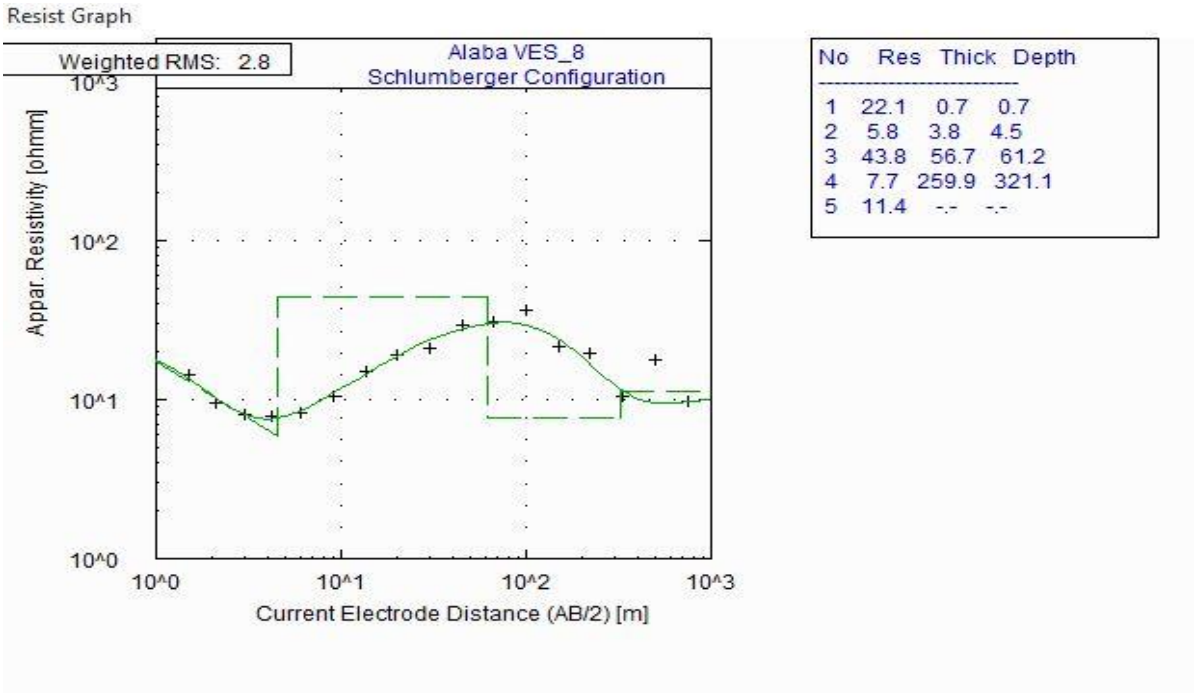
Resist Graph
Weighted RMS: 2.8
Alaba VES_8
Schlumberger Configuration
Appar. Resistivity [ohmm]
10^3
10^2
10^1
10^0
10^0
10^1
10^2
10^3
Current Electrode Distance (AB/2) [m]
No Res Thick Depth
1 22.1 0.7 0.7
2 5.8 3.8 4.5
3 43.8 56.7 61.2
4 7.7 259.9 321.1
5 11.4 -.- -.-

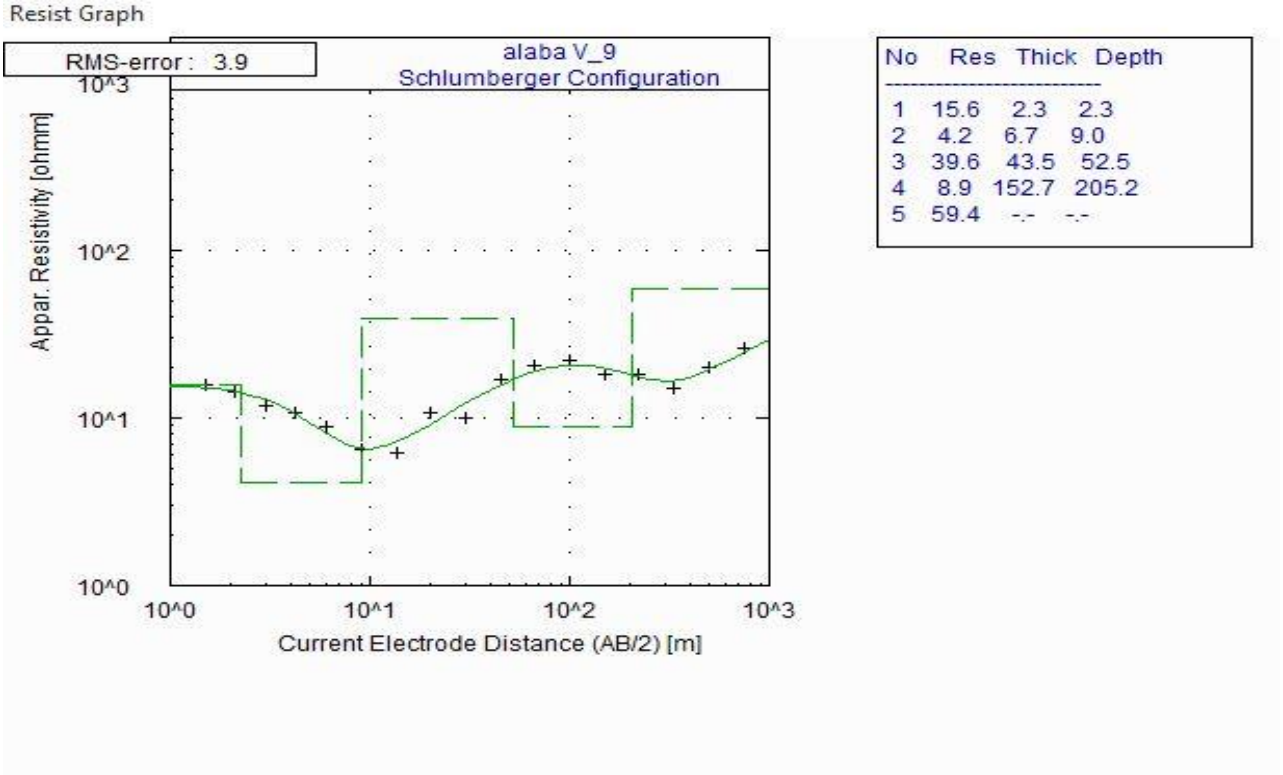
Resist Graph
RMS-error : 3.9
alaba V_9
Schlumberger Configuration
Appar. Resistivity [ohmm]
10^3
10^2
10^1
10^0
10^0
10^1
10^2
10^3
Current Electrode Distance (AB/2) [m]
No Res Thick Depth
1 15.6 2.3 2.3
2 4.2 6.7 9.0
3 39.6 43.5 52.5
4 8.9 152.7 205.2
5 59.4 -.- -.-

Appendix 2: lithological description of borehole data from South water construction enterprise

Location
398425E, 810279N 1762m

Depth (m)	Description
0 -4	Brown clay
and4 -8	Slightly weathered ignimbrite
8 - 26	Fresh ignimbrite
26 -28	Tuff
28 -40	Pyroclastic fragment
40 -44	Ignimbrite
44 -52	Ash
52 -70	Fractured ignimbrite
70 -122	Pumice
122 -128	Pumice with sand
128 -134	Tuff with sand
134 -148	Sand with pumice